MICRO SCALE ENERGY HARVESTING FOR

ULTRA-LOW POWER SYSTEMS

Hafeez KT

A Thesis Submitted to

Indian Institute of Technology Hyderabad

In Partial Fulfillment of the Requirements for

The Degree of Master of Technology

भारतीय प्रौद्योगिकी संस्थान हैदराबाद

Indian Institute of Technology Hyderabad

Department of Electrical Engineering

June 2011

Declaration

I declare that this written submission represents my ideas in my own words, and where ideas or words of others have been included, I have adequately cited and referenced the original sources. I also declare that I have adhered to all principles of academic honesty and integrity and have not misrepresented or fabricated or falsified any idea/data/fact/source in my submission. I understand that any violation of the above will be a cause for disciplinary action by the Institute and can also evoke penal action from the sources that have thus not been properly cited, or from whom proper permission has not been taken when needed.
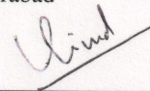
(Signature)

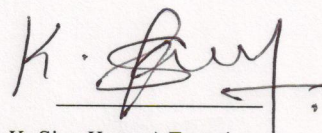Hafeez- KT

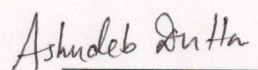(– Student Name –)

EE09G004

(Roll No.)

Approval Sheet

This Thesis entitled MICRO SCALE ENERGY HARVESTING FOR ULTRA-LOW POWER SYSTEMS by Hafeez KT is approved for the degree of Master of Technology from IIT Hyderabad
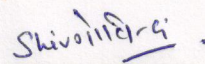

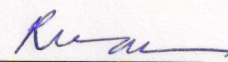(Dr. Vinod Janardhanan) Examiner
Dept. of Chem Eng
IITH

(Dr. K. Siva Kumar) Examiner
Dept. Elec Eng
IITH

(Dr. Ashudeb Dutta) Adviser 1
Dept. of Elec Eng
IITH

(Dr. Shiv Govind Singh) Adviser 2
Dept. of Elec Eng
IITH

(Dr. Ravindra N. Guravannavar) Chairman
Dept. of Comp Eng
IITH

Acknowledgements

Abstract

Ultra-low power systems such as Wireless sensor network (WSN) nodes have emerged as an active research topic due to their vast application areas. Such WSNs would be able to perform their sensing functions and wireless communication without any supervision, configuration, or maintenance. These systems have to cope with severe power supply constraints. The need shared by most WSNs for long lifetimes and small form factors does not match up well with the power density of available battery technology. This could limit the use of WSNs due to the need for large batteries. It is not expected that better batteries for small devices will become available in the near future. Energy harvesting could therefore be a solution to making WSNs autonomous and could thus enable widespread use of these systems in many applications. Energy harvesting is becoming more and more popular for micro-power applications where the environmental energy is used to power up the systems.

As sensors have become smaller, cheaper, and increasingly abundant, there have been commensurate reductions in the size and cost of computation and wireless communication. In context of micro scale solar energy harvesting systems, the design of efficient energy conversion unit and accurate maximum power point tracking(MPPT) unit becomes a tremendous challenge due to area constraint and very low ($\sim\mu$W) output power. This thesis presents a novel MPP tracking method including a charge pump based DC-DC converter for extracting energy from a tiny single PV cell (open circuit voltage $\sim$0.4V). We have used a feed-forward (FF) unit to track maximum power point. The design of FF MPP is derived from the operating point of solar cell under different solar intensity. This scheme consumes very little power and is faster when compared to other methods. This method eliminates the use of current sensor and other power hungry elements in the MPPT unit. The proposed method tracks the MPP with less than 2 % error and gives efficiency of 63.50% through FF MPPT. The complete circuit has been simulated using 0.18 μm CMOS process.

Contents

Chapter 1

Introduction

1.1 Introduction

Rapid advances in Nano scale integration have open new class of ultra-low power miniaturized electronic systems. These ultra-low power systems are gaining more attention due to their vast application areas such as smart dust sensors [1], biomedical implants [2]. Usually these devices are powered by batteries and hence their lifetime is limited. Replacement of battery is not easy because of infeasibility (biomedical implant) and high cost (large wireless sensor network). Environmental energy harvesting is found to be an effective solution to these systems so that they can work for several months or years without battery replacement[3, 4].

Solar energy is most effective among the available environmental energy sources due to its high energy density [5, 6]. The output voltage of a single Photo-Voltaic (PV) cell is generally below 0.4V that is often too low to drive any analog system [7]. Therefore multiple PV cells are stacked in series to obtain higher output voltage. However, such configuration may not be viable in micro-scale systems due to size and packaging constrains [8]. Therefore a single solar PV cell has shown potential solution to extract the power in micro scale system in order to minimize the area and cost of the system.

The output power of solar cell depends on light intensity and connected load [9]. Output power is zero if the solar cell is short circuited (zero load) and open circuited (infinite load). The optimal operating point of solar cell for maximum power transfer exists in between these points. Optimum operating point is achieved through the impedance matching of PV cell and system load. This technique is called Maximum power point tracking (MPPT). The MPP tracking and power management of large solar array is well studied and developed [10]. However, designing of such circuits for single solar cell introduces new challenges as the output voltage is comparable to or less than the threshold voltage of MOSFET at 0.18 μm CMOS technology [8, 11].

In a standard solar cell driven system, storage batteries or super capacitors are used to store energy from solar cell, so that the device can work even in the absence of sun light. The storage batteries normally work on or above 1V [12]. Therefore, the output voltage (0-0.4V) of the single PV cell needs to be stepped up before storing in batteries. A DC-DC converter and a MPPT (maximum power point tracking) system are used to step up the voltage and to ensure MPP operation of solar cell in all light intensities. Since the power obtained from a single solar cell is very less, the most significant design consideration for this system is to ensure minimum power consumption. To tackle this challenge we are proposing a novel Maximum Power Point Tracking topology, to maximize harvested energy from solar cell.

1.2   Aim and Motivation

During the last decade, research in ultra-low power systems has opened numerous applications. Some examples of applications include defense networks that could be rapidly deployed by unmanned aerial vehicles (UAV), tracking the movements of birds, small animals, and even insects, fingertip accelerometer virtual keyboards, monitoring environmental conditions affecting crops and livestock, inventory control, and smart office spaces. In most of these applications the system should be completely wireless and autonomous. Conventional systems use batteries to power the devices and hence the lifetime of the device is limited. Providing perennial power to these devices is an active area of research now a day. Pushing forward the frontiers of system integration, miniaturization, and energy consumption, designing an autonomous solar powered IC is the aim of this project.

1.3   Literature Survey in brief

Even though the solar energy harvesting for high power systems are well developed, research on solar power scavenging for low power systems like sensor networks is gaining more attention nowadays. Prometheus [13] and Heliomote [14]were probably the first proposals to supply a sensor node with the help of a small PV module. Both systems do not perform any MPPT and the refill of energy buffers is performed by a direct connection between the PV panel and the storage device. Simjee and Chou proposed an MPPT system that uses a super capacitor as energy reservoir [15]. The micro-controller on the node runs a tracking algorithm and drives a pulse width modulator (PWM) circuit to control the power converter. Ambimax [16] is another solution from the same authors of [15]. It is a more refined version and tries to eliminate the overhead caused by an always-running algorithm on the micro controller unit.

Kobayashi et al used fractional open circuit voltage (FOC) method [17] for MPPT. It uses the approximate linear relation between open circuit voltage and MPP voltage(V_{MPP}). The disadvantage of this method is that frequently disconnecting PV cells from the load causes power loss and requires circuit for time multiplexing. An improved design was proposed by D. Brunelli, L. Benini [18] which eliminates the power loss due to frequent disconnecting the PV cell from load by adding a tiny PV cell. This tiny PV cell is used to calculate the V_{MPP}.

Shao.et al [19] implemented Hill climbing algorithm using dedicated hardware to suite low power applications. This circuit performs well for high voltage- low current systems (3V, 180μA) where the switching frequency of the power converter can be low (eg: around 2 MHz). Hill climbing algorithm may malfunction in the case of multiple solar cells due to the presence of local maxima generated by partial shading. In low voltage-high current systems using single solar cells (0.4V, 500μA), the switching frequency requirement of power converter will be high of the order of 10-20MHz [20]. The current sensor for switching power converters proposed by H. Y. H. Lam.et al [21] can operate effectively only if the switching frequency is on or below 500KHz. Du and Lee proposed another method, which can work effectively up to 2MHz [22].These literature surveys suggest that design of current sensing circuit for 10-20MHz frequencies is very difficult. Hence, MPP tracking is not possible by using current sensing based hill climbing method. Recently Lu.et al [23] has proposed alternative theoretical MPP tracking method based on the analysis of the characteristics of solar cell and charge pump. This method needs prior characterization of solar cell and the charge pump. However the hardware implementation of this method will be very complex and difficult. Therefore in this thesis we propose an empirical method to overcome the hardware complexity. That will resulted in high

accuracy MPP tracking for ultra-low power system.

1.4 Contribution of the Thesis

This work focuses on the design and implementation of solar energy harvesting system for ultra-low power systems. The main contributions of this research work are as follows:

- A comprehensive analysis of the key performance parameters of charge pumps.

- A comprehensive study of MPPT methods.

- Thorough Analysis of hill climbing based MPPT method for low power systems.

- A novel, power efficient method for the sizing of MOSFETs in the charge pump design.

- A novel, feed forward method for the design of MPPT system for micro scale energy harvesting systems.

1.5 Brief Overview of the Thesis

A brief overview of the thesis is presented here.

1.5.1 Energy harvesting for ultra-low power applications

There is a pressing need for the design of ultra-low power, self-powering circuit for a number of applications such as remote wireless sensor nodes or biomedical implant (artificial eye implant). As these require small area, it is essential to generate power from a single-solar cell that will force the researcher to build up an ultra-low voltage power management circuit. Solar energy harvesting is found to be a good solution to power these devices.

A typical solar energy harvesting system consists of a solar cell, DC-DC converter, control unit and battery storage (energy buffer). The solar cell converts light energy to electrical energy that has been stored in a storage batteries or super capacitors. The storage batteries normally function on or above 1V. However, due to very low output voltage of single solar cell (0-0.4V), a DC-DC converter based power management unit is placed in-between solar cell and batteries to step up the solar output voltage.

The literature [20, 24] suggest in single solar cell energy harvester, for fully on-chip realization perspective, the charge pump based DC-DC converter become better choice for boosting the voltage compare to inductor based DC-DC converters. Power transferred from solar cell to charge pump is maximum if their impedance is matched. However, impedance of the solar cell changes with light intensity, hence to ensure maximum power transfer, the impedance of the charge pump also must change. This is achieved using the control unit by varying the frequency of the charge pump. The control unit finds the optimum frequency using MPPT algorithms.

In micro scale energy harvesting systems the power loss in power converter (charge pump) and the MPPT circuit are comparable to the harvested power. Hence we can't neglect these power losses during the design of the system. Additionally these losses depend on the operating point of the power converter. Therefore, just maximizing the output power of PV cell alone cannot give optimal solution. Hence the design of micro scale energy harvesting requires comprehensive modeling and analysis of solar cell and charge pump.

1.5.2 Analysis of hill climbing based MPPT method for low power systems

In single solar cell system, PV cell stacking is absent. Hence, partial shading is not considerable. Therefore local maxima will not appear in the characteristics. For such systems, Hill climbing / perturb and observe methods are preferable for MPP tracking. Circuit implementation [19] of this algorithm consists of a current sensor, a comparison block and a decision making block. Since the output voltage of charge pump is almost fixed, the output power is maximized by maximizing output current by varying the Switching frequency of charge pump. In this design charge pump steps up the voltage from the solar cell and MPPT unit monitors the charge pump output power using current sensor and determines the adjustment of the system operating parameter. Based on the adjustment decision, the operating frequency of the charge pump is tuned in order to maximize the system power output.

In single PV cell system, the output voltage is very low. Therefore we need to get more current to meet the power requirements of standard applications. To transfer high amount of current the switching frequency of the charge pump should be high. The output of the charge pump is connected to current sensor to measure the current. The existing current sensor topology cannot perform in high switching frequency because of the limited gain bandwidth product [22]. If we go for high frequency operation, the stability gets affected. This has been verified through simulation. Therefore to implement hill climbing algorithm for these system requires a modification of the current sensor. Current sensor design for high frequency may become complicated and power consuming. So the design challenge is to implement hill climbing algorithm without using current sensor or we have to modify the current sensor circuit for high frequency and low power applications.

1.5.3 Power efficient method for the sizing of MOSFETs in the charge pump design

Charge pump steps up the input voltage by sharing the charge between capacitors through MOSFET switch [25]. There is multiple charge sharing paths in series or parallel depending on the configuration. The ON resistance of the MOSFETs varies from one charge sharing path to another path. This happens because ON resistance depends on the voltage across the MOSFET and the voltage level is different for different charge sharing paths [20]. Existing charge pump design uses same MOSFET sizes in all the charge sharing paths [26]. However this choice (same size to all the switching MOSFET) is not power efficient in micro scale energy harvesting system. Therefore we have proposed that non uniform sizing of the switching MOSFET across various charge sharing paths can save significant amount of power. In this work, MOSFET sizes have been optimized individually for power efficient operation.The proposed method gives an additional power gain around 20μW.

1.5.4 Feed forward method for the design of MPPT system for micro scale energy harvesting

In this section we have propose a novel MPP tracking method for efficient energy harvesting. The basic aim of the proposed method is to derive the information about optimum frequency of charge pump from the operating point of solar cell. Since the output of the solar cell is fed to the charge pump, in this approach, a combined I-V characteristic (including the losses) of the solar cell and charge pump has been extracted. By using these characteristics, it is possible to relate the optimum operating point of the charge pump to the output voltage of the solar cell (V_{OP}). This is equivalent to the computation of optimum clock frequency to

charge pump based on solar output voltage. Therefore, we can conclude that it can be represented as a voltage control oscillator (VCO), because it is basically a voltage -frequency relationship.

In our design, first find the optimum operating frequency of charge pump (at MPP) for different light intensities by manually varying the clock frequency and extract the corresponding solar operating voltage (V_{OP}). Then we can design an equivalent VCO that will match the relationship of V_{OP} and optimum frequency. This VCO is connected in between solar cell and charge pump for MPP tracking. The proposed method tracks the MPP with less than 2 % error and gives efficiency of 63.50% through FF MPPT. The complete circuit has been simulated using 0.18 μm CMOS process.

1.6   Thesis Organization

This thesis is organized into following chapters.

- Chapter 1: is the introduction describing the motivation behind the work, literature survey, objectives and contributions of the present work.

- Chapter 2: explores ultra-low power system and highlights the importance of energy harvesting for powering these devices.

- Chapter 3: describes solar energy and its properties. It discuss about solar cell and its parameters also.

- Chapter 4: describes ultra-low power MPPT concept and MPPT methods.

- Chapter 5: describes design and performance of charge pump circuits and analyzes the losses in it.

- Chapter 6: describes design and performance of Hill climbing based MPPT method implementation and its draw backs.

- Chapter 7: describes design and performance of a novel feed forward technique for energy harvesting.

- Chapter 8: presents the conclusion to the thesis as well as future directions of this work.

Chapter 2

Energy harvesting for wireless systems

2.1 Introduction

Advances in hardware technology and engineering design have led to dramatic reductions in size, power consumption and cost for digital circuitry, wireless communications and Micro Electro Mechanical Systems (MEMS). A new class of devices has emerged as a result of these technology advancements collectively called as ultra-low power wireless systems. These advancements make it possible to integrate sophisticated functions into a single micro-power ubiquitous system, which can be used in applications such as PicoRadio [27], wireless sensor node and biomedical implantable devices [2, 28, 29]. These applications demand compact volume, low cost, long lifetime and high integration. One of the design challenges is to provide the required power supply. The size of the application limits the capacity of the battery and thus the operation time of the system [30]. While there are many obvious short-term advantages of using batteries, they do have a long-term negative environmental impact. More over replacing the batteries may not be possible because of expense (large WSN) or practical difficulties (battlefield, medical implants as in Fig 2.1). An alternative to batteries exists in harnessing the ambient energy surrounding the system and subsequently converting it into electrical energy. Once a long-established concept, energy harvesting offers an inexhaustible replacement for batteries. Energy-harvesting systems scavenge power from optical, acoustic, thermal, and mechanical energy sources. The proliferation of and advances in wireless technology, particularly wireless sensor nodes and mobile electronic devices, has increased the volume of energy harvesting research as of late. This thesis reviews the principles of the state of the art in energy harvesting systems. We focus on generating electrical power from solar energy because it's high energy density and free availability.

2.2 Wireless sensor networks

2.2.1 Introduction

A wireless sensor is simply a device that monitors an input and then sends information using either radio waves or infrared light. A typical wireless sensor node contains sensors, wireless communication module and power source (usually battery). Wireless sensor network consist of numerous wireless sensor nodes functioning together for a specific purpose as shown in Fig 2.2. "A wireless sensor network (WSN) is a wireless network consisting of spatially distributed autonomous devices using sensors to cooperatively monitor
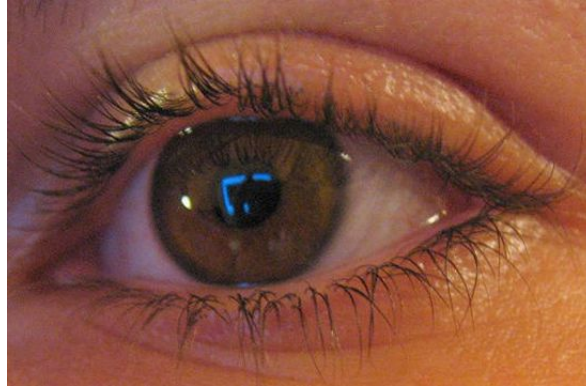
Figure 2.1: Solar powered retinal implant

physical or environmental conditions, such as temperature, sound, vibration, pressure, motion or pollutants, at different locations."(wikipedia).

Wireless sensor networks have found numerous applications in wide areas. They are widely used as defense networks that could be rapidly deployed by unmanned aerial vehicles (UAV). Other applications include whether forecasting, tracking the movements of birds, small animals, and even insects, fingertip, monitoring environmental conditions affecting crops and livestock, inventory control, and smart office spaces. They are used by the warfighter to enhance wide area surveillance and situation understanding. Through coordinated monitoring of environmental conditions such as temperature, pressure, sound, or vibration, sensors can provide significant battlefield information. Wireless sensors can also be used for condition based maintenance (CBM) on Navy ships [31].

Both the sensors and communication module require power for their operation. Historically, batteries have supplied power to these micro systems. Hence their life time is limited. Moreover, for many applications, it is impossible to replace the batteries after they are depleted, and the systems become useless afterwards.

2.2.2 Finite Power

Nowadays most of the low power portable devices are battery powered. The number of functional modules integrated in a device is increasing and hence the power requirements also increase. Since the size of these devices are shrinking and the area dedicated to the energy buffer (battery) is limited. Even though the battery technology is developing, it is not fast enough to satisfy the power requirements. Power management is an active area in circuit design because of this finite power. No advances in chemical cell technology will completely eliminate its inherent physical limitation of finite power. As such, finite power dominates design considerations of all battery-operated wireless sensor nodes and mobile devices. Despite energy efficient protocols and system partitioning [32], this dependency requires that batteries of a wireless microsystem be recharged or replaced. As wireless microsystems continue to grow in ubiquity, so too will battery density and labor costs. Equally, if not more important, the environmental impact of discarding potentially millions of coin-size and bigger batteries becomes irreversible.

2.2.3 Need for infinite power

Wireless sensor nodes and mobile electronic devices are increasingly becoming the obvious choice for remote data collection and context recognition. Applications for these microsystems extend well beyond monitoring

7
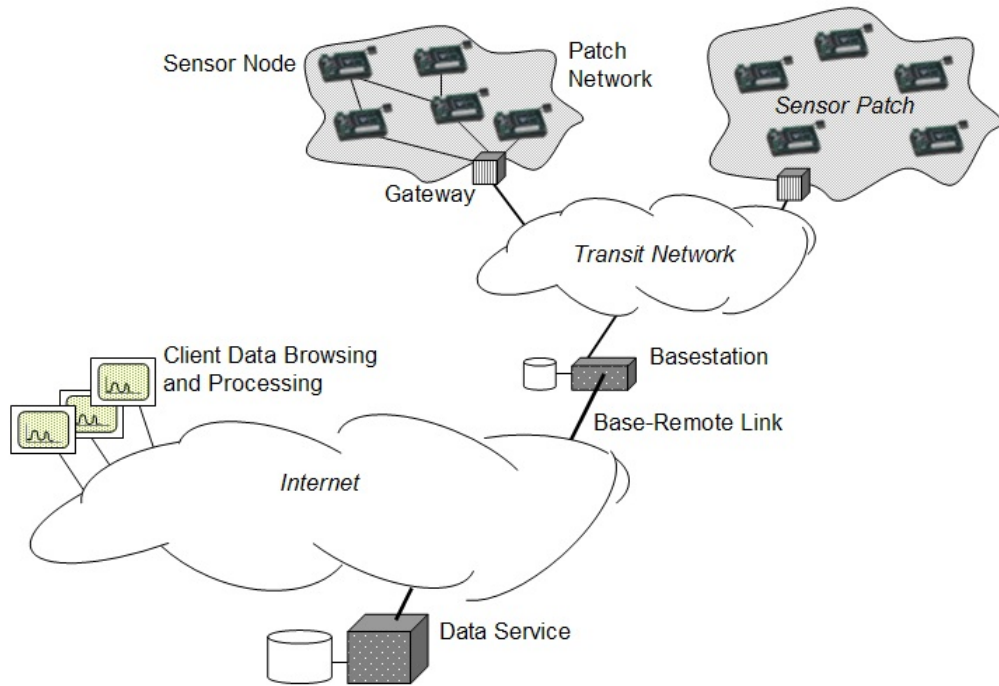
Figure 2.2: Typical wireless sensor network

temperature, location, material fatigue and chemical detection. These systems play a particularly vital role in biomedical electronics and wearable computing. The life time of these devices are limited because of the battery. We present two case studies to illustrate the same.

2.2.4 Case study: Great duck island project

Great Duck Island is a 237-acre island located off the coast of Maine and an important nesting ground for Leach's Storm Petrel, a common New England seabird. In spring 2002, the College of the Atlantic, in collaboration with the University of California, Berkeley, and Intel Corp., deployed a sensor network consisting of 32 motes on the island to monitor the Petrel's nesting behavior. Using a sensor network allowed scientists to continually measure environmental data in and around the Petrel's nesting burrows without disturbing the nesting birds [33] as shown in Fig 2.3. Biologists put sensor devices in the underground nests of the storm petrel (1) and on 4-inch stilts placed just outside their burrows (2). These devices record data about the birds and relay it, bucket-brigade style, to a gateway node (3), which transmits the info to a laptop in the research station (4), then to a satellite dish (5) and, ultimately, to a lab in California. Over a three-month period during summer 2002, the sensor network delivered 1.8 million measurement packets to its base station, with individual motes delivering up to 50,000 packets. Each mote was programmed to measure several environmental variables including temperature, humidity, barometric pressure, and light level.

The specifications of the nodes are given in the Table 2.1. From the table it is clear that the life time of the project was limited because of battery.

8

Figure 2.3: Sensor nodes in the Great Duck Island project

Table 2.1: Specifications of Great Duck Island project

specification	value
Sampling Rate	$8.33 \times 10^{-4}\ H_z$
TX Rate	0.03 B/s
Power Consumption	1.6 mW
Battery Capacity	860mAh
Lifetime	63 days

2.2.5 Case study : Golden gate bridge project
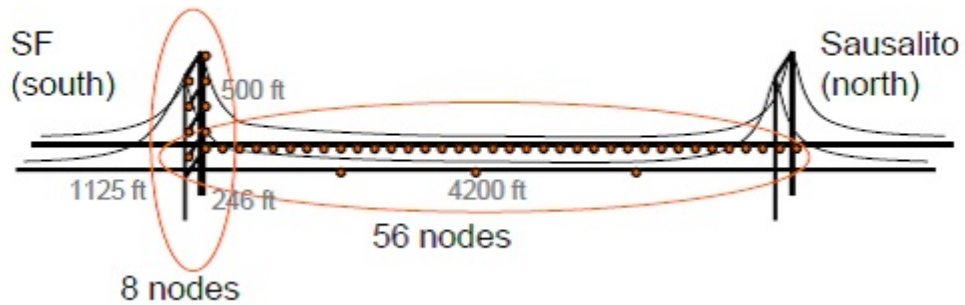
Figure 2.4: The golden Gate Bridge and layout of nodes on the bridge.

A Wireless Sensor Network (WSN) for Structural Health Monitoring (SHM) is designed, implemented, deployed and tested on the 4200ft long main span and the south tower of the Golden Gate Bridge (GGB) [34] as shown in Fig 2.4. The aim of the golden gate bridge project was to Estimate the state of structural health, or detecting the changes in structure that affect the performance. Ambient structural vibrations are reliably measured at a low cost and without interfering with the operation of the bridge. Requirements that SHM imposes on WSN are identified and new solutions to meet these requirements are proposed and

implemented. In the GGB deployment, 64 nodes are distributed over the main span and the tower, collecting ambient vibrations synchronously at 1 KHz rate, with less than 10μs jitter, and with an accuracy of 30uG. The sampled data is collected reliably over a 46-hop network, with a bandwidth of 441B/s at the 46th hop. The collected data agrees with theoretical models and previous studies of the bridge. The deployment is the largest WSN for SHM. The specifications are shown in Table 2.2

Table 2.2: Specifications of Golden Gate Bridge project

specification	value
Sampling Rate	$1KH_z$
TX Rate	441 B/s
Power Consumption	358.2 mW - 672.3 mW
Battery Capacity	4 x 18000mAh at 6V
Lifetime	35 days

2.3   Available energy sources

Figure 2.5 offers a decisive comparison of vibration-based and solar energy versus conventional battery power. The darkest shade depicts exclusively vibration-based energy while the lesser shaded region represents both indoor and direct photovoltaic energy generation.
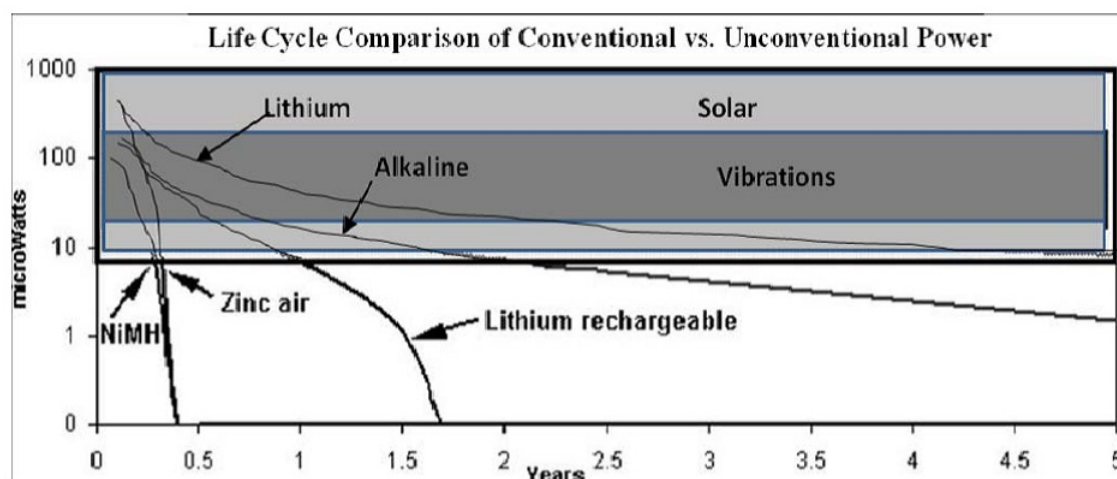
Figure 2.5: Comparison of power Densities (from [35])

It is possible to deduce from Fig 2.5 that design consideration should include the projected lifetime of the electronic application. If the design is to be utilized for only a few years, one could argue that batteries provide the simplest and most adaptable power source. However, the availability of adequate environmental light energy demands consideration as a solution. Nonetheless, should the projected lifetime extend beyond several years and light energy is not readily available, other domains of energy harvesting become attractive solutions. The available environmental energy sources and their power densities is given in Table 2.3

Hence wireless sensor nodes can be powered by using any of these available energy sources and some examples are shown in Fig 2.6. From the table it is clear that among all the available environmental energy sources, solar has the highest power density and it is freely available.

Table 2.3: Comparison of environmental energy sources (from [35])

Source	Power density (W/cm3)
Solar (outdoors)	15,000-Direct sun, 150-cloudy day
Solar (indoors)	6- office desk
Vibrations (piezoelectric conversion)	250
Vibrations (electrostatic conversion)	50
Acoustic noise	0.003 at 75 dB, 0.96 at 100 dB
Temperature gradient	15 at 10° C
Shoe inserts	330
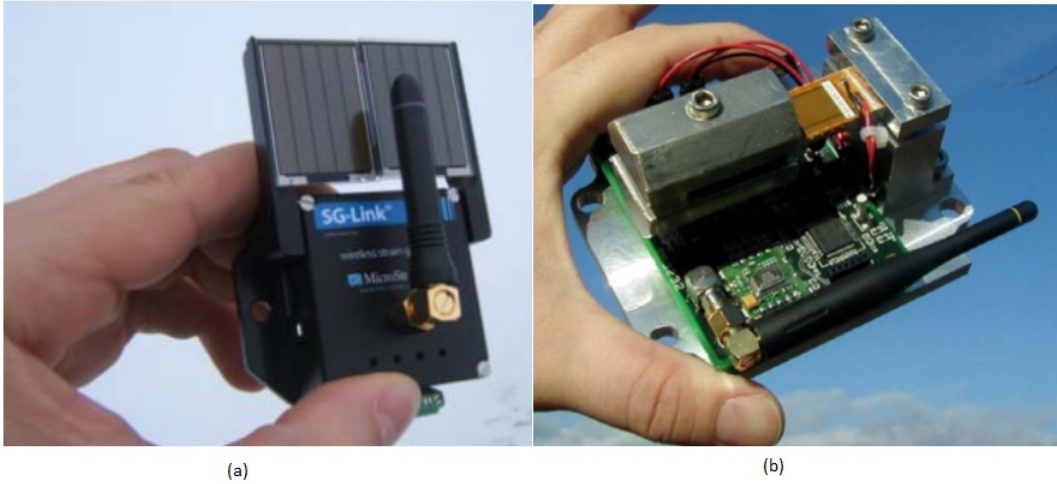
Figure 2.6: (a) Integrated solar energy harvester strain sensing node (b) Integrated piezoelectric vibration energy harvester sensing node.

2.4 Conclusion

Different environmental energy, such as solar, vibration, heat, and radioactive decay of matters, can be collected and converted to the electrical energy through different energy transducers, to power up the microsystems. Since the environmental energy exists everywhere and usually, the energy amount can be infinite, the device lifetime can be extended to virtually infinity. Selection of the suitable energy source depends on the power requirement and working atmosphere of the system. Solar energy is the best suitable energy source option for outdoor applications. The voltage generated in a solar cell is dc. Hence rectification is not needed. This will reduce the circuit complexity. Because of these advantages, in this project work solar energy is utilized as the non-conventional energy source.

Chapter 3

Solar energy

3.1 Introduction

Solar energy is derived from the radiant light or heat emitted by the sun. Solar radiation represents the most readily available renewable energy source on the planet. Of the 174 PW (174x1015 watts) that reach the Earth's upper atmosphere, approximately half penetrates to the surface of the Earth [36]. In 2005, the average global consumption of power was 15 TW (15x1012 watts) [37]. From this information we can easily deduce that the sun provides far more power than the world could ever use in the near future. There are many ways to use the solar energy such as heat and electricity. Solar radiation is directly converted to electricity using device called photovoltaic cells or solar cells.

The first practical photovoltaic devices demonstrated in the 1950s. Research and development of photo voltaic received its first major boost from the space industry in the 1960s which required a power supply for satellite applications. In the 1980s research into silicon solar cells paid off and solar cells began to increase their efficiency. In 1985 silicon solar cells achieved the milestone of 20% efficiency. The year 1997 saw a growth rate of 38% and today solar cells are recognized not only as a means for providing power and increased quality of life to those who do not have grid access, but they are also a means of significantly diminishing the impact of environmental damage caused by conventional electricity generation in advanced industrial countries [38].

3.2 Solar cell operational principle

A solar cell is an electronic device which directly converts sunlight into electricity. Light shining on the solar cell produces both current and voltage to generate electric power. The "photovoltaic effect" is the basic physical process through which a PV cell converts sunlight into electricity. This process requires firstly, a material in which the absorption of light raises an electron to a higher energy state, and secondly, the movement of this higher energy electron from the solar cell into an external circuit. The electron then dissipates its energy in the external circuit and returns to the solar cell. A variety of materials and processes can potentially satisfy the requirements for photovoltaic energy conversion, but in practice nearly all photovoltaic energy conversion uses semiconductor materials in the form of a p-n junction [39].

Figure 3.1: Solar cell

3.3 Solar cell structure

Solar cells basically consist of p-type and n-type semiconductors with two metal contacts, one in p-type and the other in n-type as shown in Fig. 3.2. These two types of semiconductors form a p-n junction with n-type facing the sun. Sunlight is composed of photons containing energy which correspond to the different wavelengths of the solar spectrum. When photons strike a solar cell, depending upon the type of semiconductor used some low energy photons (infrared) are not absorbed by the electrons in the semiconductor material while some high energy photons are absorbed for excitation of electrons into the conduction band and the excess of energy is released as heat. These excited electrons are attracted toward the n-type semiconductor. This causes more negative charges in the n-type and more positive charges in the p-type semiconductors. If an electric load is connected between the two types of semiconductors through the metal contacts, electrons start flowing from n-type to p-type semiconductors via the load. Thus photon energy is directly converted to electrical energy without an intermediate mechanical or thermal process.

3.4 The Photovoltaic Effect

In order to generate power, a voltage must be generated as well as a current. Voltage is generated in a solar cell by a process known as the "photovoltaic effect". The collection of light-generated carriers by the p-n junction causes a movement of electrons to the n-type side and holes to the p-type side of the junction. Under short circuit conditions, there is no buildup of charge, as the carriers exit the device as light-generated current.

However, if the light-generated carriers are prevented from leaving the solar cell, then the collection of light-generated carriers causes an increase in the number of electrons on the n-type side of the p-n junction and a similar increase in holes in the p-type material. This separation of charge creates an electric field at the junction which is in opposition to that already existing at the junction, thereby reducing the net electric field.

13

Figure 3.2: Solar cell structure

Since the electric field represents a barrier to the flow of the forward bias diffusion current, the reduction of the electric field increases the diffusion current. A new equilibrium is reached in which a voltage exists across the p-n junction. Under open circuit conditions, the forward bias of the junction increases to a point where the light-generated current is exactly balanced by the forward bias diffusion current, and the net current is zero. The voltage required to cause these two currents to balance is called the "open-circuit voltage".

3.5 Light Generated Current

The generation of current in a solar cell, known as the "light-generated current", involves two key processes. The first process is the absorption of incident photons to create electron-hole pairs. Electron-hole pairs will be generated in the solar cell provided that the incident photon has energy greater than that of the band gap. However, electrons (in the p-type material), and holes (in the n-type material) are meta-stable and will only exist, on average, for a length of time equal to the minority carrier lifetime before they recombine. If the carrier recombines, then the light-generated electron-hole pair is lost and no current or power can be generated.

A second process, the collection of these carriers by the p-n junction, prevents this recombination by using a p-n junction to spatially separate the electron and the hole. The carriers are separated by the action of the electric field existing at the p-n junction. If the light-generated minority carrier reaches the p-n junction, it is swept across the junction by the electric field at the junction, where it is now a majority carrier. If the emitter and base of the solar cell are connected together (i.e., if the solar cell is short-circuited), the light-generated carriers flow through the external circuit.

3.6   Collection Probability

The "collection probability" describes the probability that a light generated carrier absorbed in a certain region of the device will be collected by the p-n junction and therefore contribute to the light-generated current, but probability depends on the distance that a light-generated carrier must travel compared to the diffusion length. Collection probability also depends on the surface properties of the device. The collection probability of carriers generated in the depletion region is unity as the electron-hole pair is quickly swept apart by the electric field and are collected. Away from the junction, the collection probability drops. If the carrier is generated more than a diffusion length away from the junction, then the collection probability of this carrier is quite low. Similarly, if the carrier is generated closer to a region such as a surface with higher recombination than the junction, then the carrier will recombine.

3.7   Quantum efficiency

The "quantum efficiency" (Q.E.) is the ratio of the number of carriers collected by the solar cell to the number of photons of a given energy incident on the solar cell. The quantum efficiency may be given either as a function of wavelength or as energy. If all photons of a certain wavelength are absorbed and the resulting minority carriers are collected, then the quantum efficiency at that particular wavelength is unity. The quantum efficiency for photons with energy below the band gap is zero. A quantum efficiency curve for an ideal solar cell is shown in Fig 3.3. While quantum efficiency ideally has the square shape shown above, the quantum efficiency for most solar cells is reduced due to recombination effects. The same mechanisms which affect the collection probability also affect the quantum efficiency. For example, front surface passivation affects carriers generated near the surface, and since blue light is absorbed very close to the surface, high front surface recombination will affect the "blue" portion of the quantum efficiency. Similarly, green light is absorbed in the bulk of a solar cell and a low diffusion length will affect the collection probability from the solar cell bulk and reduce the quantum efficiency in the green portion of the spectrum. The quantum efficiency can be viewed as the collection probability due the generation profile of a single wavelength, integrated over the device thickness and normalized to the incident number of photons. The "external" quantum efficiency of a silicon solar cell includes the effect of optical losses such as transmission and reflection. However, it is often useful to look at the quantum efficiency of the light left after the reflected and transmitted light has been lost. "Internal" quantum efficiency refers to the efficiency with which photons that are not reflected or transmitted out of the cell can generate collectable carriers. By measuring the reflection and transmission of a device, the external quantum efficiency curve can be corrected to obtain the internal quantum efficiency curve.

3.8   Solar Cell Parameters

3.8.1   The IV curve

The IV curve of a solar cell is the superposition of the IV curve of the solar cell diode in the dark with the light-generated current. Terminal voltage is only weakly dependent on light radiation, while the current intensity increases with higher luminosity. The current voltage relation of a solar cell is given as Eq 3.1. and the plot is shown in Fig 3.4.
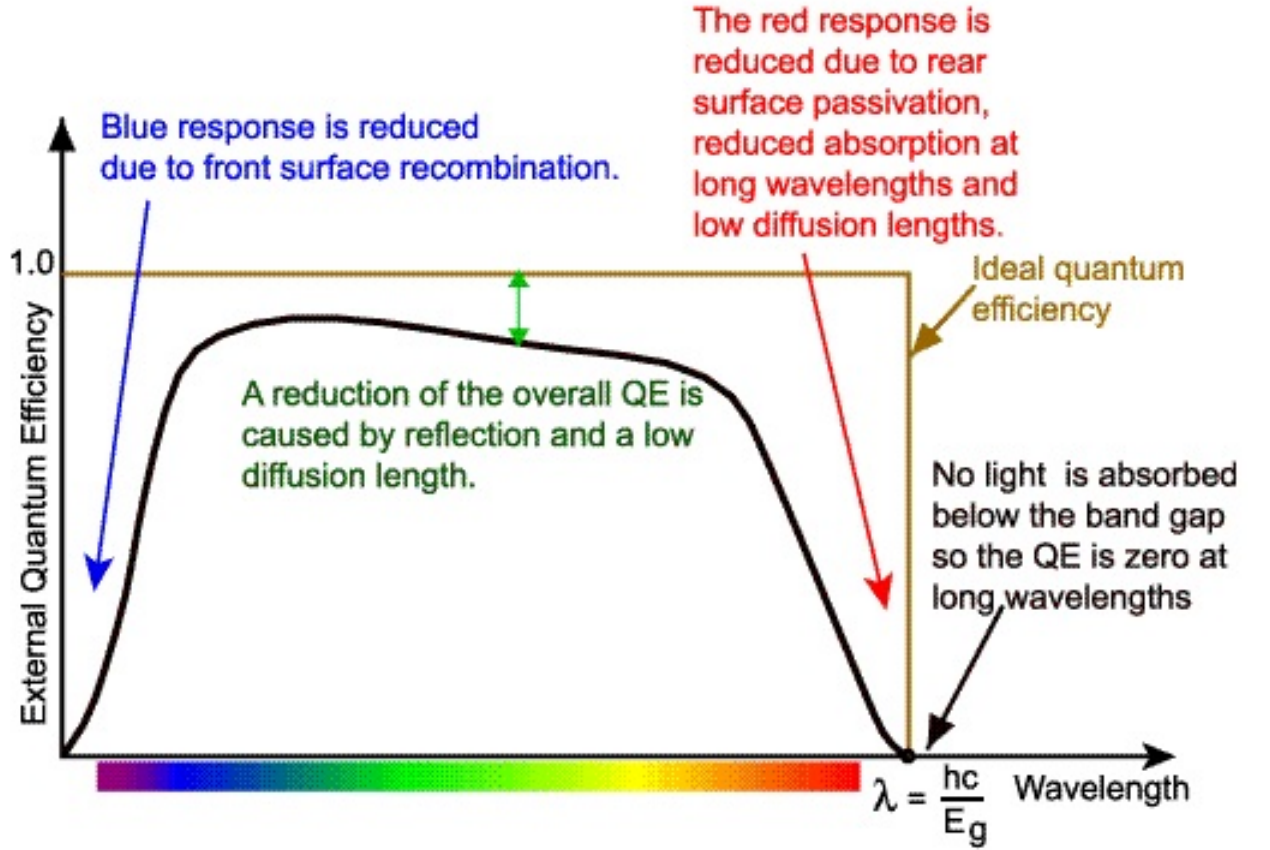
Figure 3.3: The quantum efficiency of a silicon solar cell (from [40])

$$V = \frac{nKT}{q} l_n\left(\frac{I_L - I}{I_0} + 1\right) \qquad (3.1)$$

Where n = ideality factor, q = absolute value of electron charge, K = Boltzmann's constant, and T = absolute temperature (K).

3.8.2   Short-Circuit Current

The short-circuit current is the current through the solar cell when the voltage across the solar cell is zero (i.e., when the solar cell is short circuited). Usually written as I_{SC}, the short-circuit current is shown on the IV curve in Fig 3.5. The short-circuit current is due to the generation and collection of light-generated carriers. For an ideal solar cell at most moderate resistive loss mechanisms, the short-circuit current and the light-generated current are identical. Therefore, the short-circuit current is the largest current which may be drawn from the solar cell. The short-circuit current depends on a number of factors which are described below:

- The area of the solar cell

- The number of photons (i.e., the power of the incident light source). I_{SC} from a solar cell is directly dependent on the light intensity

- The optical properties (absorption and reflection) of the solar cell and

16

Figure 3.4: I-V characteristics of solar cell
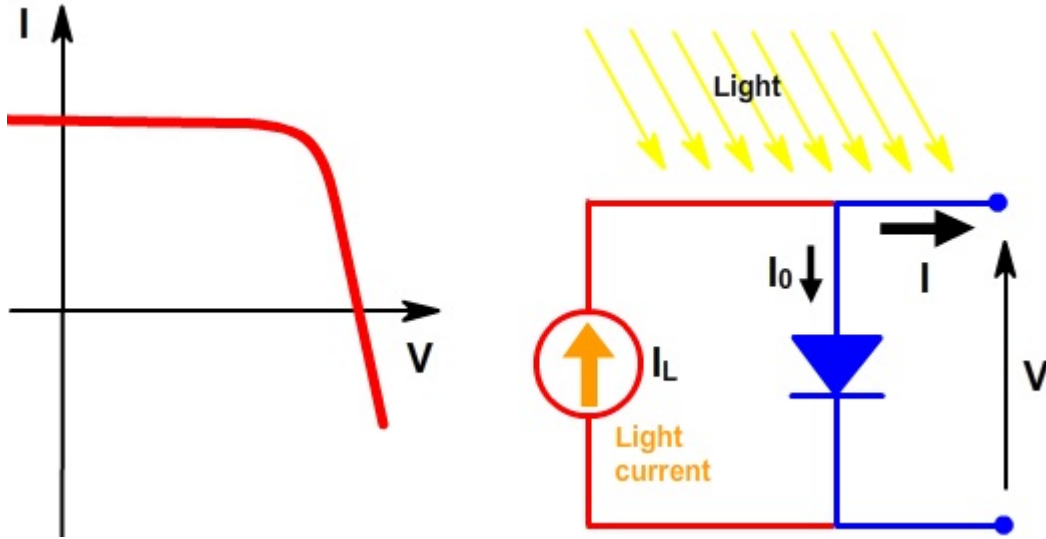
- The collection probability of the solar cell, which depends chiefly on the surface passivation and the minority carrier lifetime in the base

3.8.3 Open-Circuit Voltage

The open-circuit voltage, V_{OC}, is the maximum voltage available from a solar cell, and this occurs at zero current. The open-circuit voltage corresponds to the amount of forward bias on the solar cell due to the bias of the solar cell junction with the light-generated current. An equation for V_{OC} is found by setting the net current equal to zero in the solar cell equation and is given in Eq 3.2.

$$V_{oc} = \frac{nKT}{q} l_n\left(\frac{I_L}{I_0} + 1\right) \tag{3.2}$$

The above equation shows that V_{OC} depends on the saturation current of the solar cell and the light-generated current. While I_{SC} typically has a small variation, the key effect is the saturation current, since this may vary by orders of magnitude. The saturation current, I_O depends on recombination in the solar cell. Open-circuit voltage is then a measure of the amount of recombination in the device.

3.8.4 Maximum Power (P_{MAX})

The power produced by the cell in Watts can be easily calculated along the I-V sweep by the equation P=IV. At the I_{SC} and V_{OC} points, the power will be zero and the maximum value for power will occur between the two. The voltage and current at this maximum power point are denoted as V_{MP} and I_{MP} respectively.

3.8.5 Fill Factor

The short-circuit current and the open-circuit voltage are the maximum current and voltage respectively from a solar cell. However, at both of these operating points, the power from the solar cell is zero. The "fill factor", more commonly known by its abbreviation "FF", is a parameter which, in conjunction with V_{OC} and I_{SC},

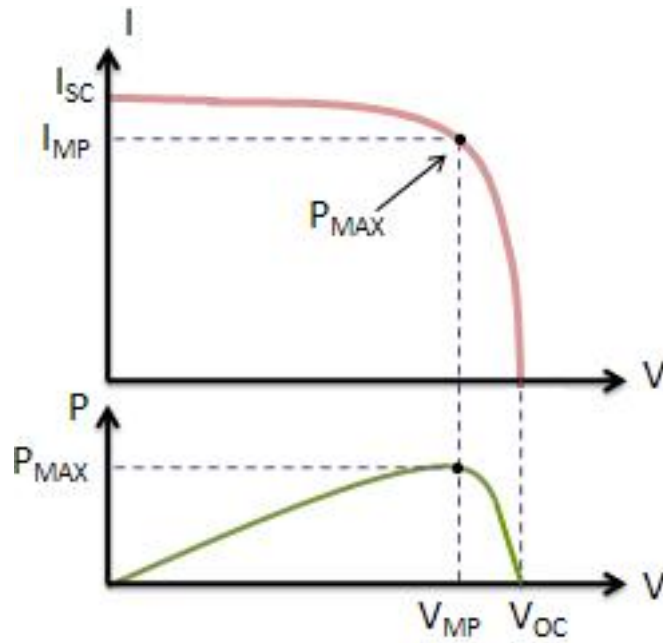Figure 3.5: Maximum Power for an I-V Sweep

determines the maximum power from a solar cell. The FF is defined as the ratio of the maximum power from the solar cell to the product of V_{OC} and I_{SC}. Graphically, the FF is a measure of the "squareness" of the solar cell and is also the area of the largest rectangle which will fit in the IV curve.
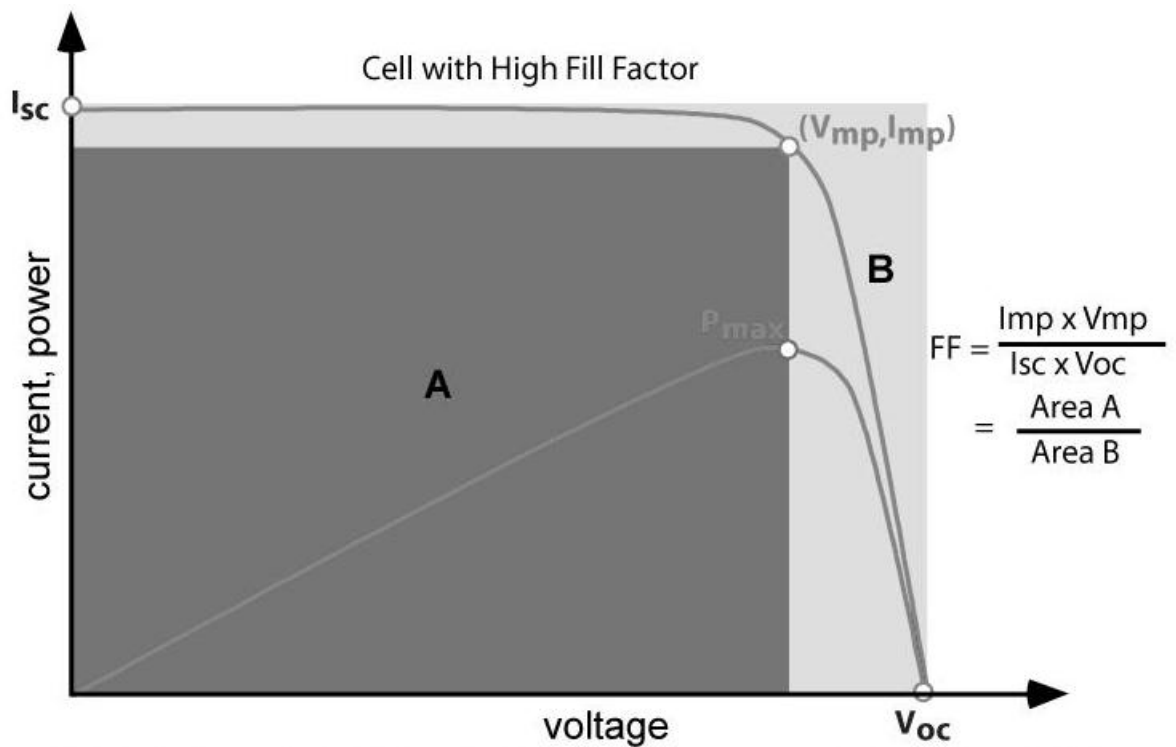

Figure 3.6: I V characteristics showing Fill factor

18

3.8.6   Efficiency

The efficiency is the most commonly used parameter to compare the performance of one solar cell to another. Efficiency is defined as the ratio of energy output from the solar cell to input energy from the sun. In addition to reflecting the performance of the solar cell itself, the efficiency depends on the spectrum and intensity of the incident sunlight and the temperature of the solar cell. Therefore, conditions under which efficiency is measured must be carefully controlled in order to compare the performance of one device to another. The efficiency of a solar cell is determined as the fraction of incident power which is converted to electricity and is defined as:

$$P_{max} = V_{oc}I_{sc}FF \tag{3.3}$$

$$\eta = \frac{V_{oc}I_{sc}FF}{P_{in}} \tag{3.4}$$

where V_{oc} is the open-circuit voltage, I_{sc} is the short-circuit current, FF is the fill factor and η is the efficiency.

3.9   Resistive effects

3.9.1   Characteristic Resistance

The characteristic resistance of a solar cell is the output resistance of the solar cell at its maximum power point. If the resistance of the load is equal to the characteristic resistance of the solar cell, then the maximum power is transferred to the load and the solar cell operates at its maximum power point. It is a useful parameter in solar cell analysis, particularly when examining the impact of parasitic loss mechanisms. The characteristic resistance is shown in the Fig 3.7
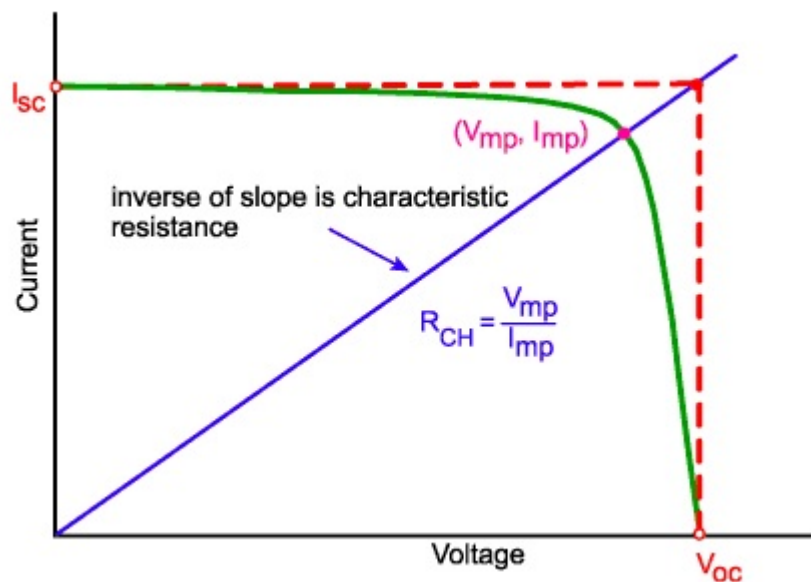

Figure 3.7: Characteristic resistance

The characteristic resistance of a solar cell is the inverse of the slope of the line, shown in the figure above can be given as:

$$R_{CH} = \frac{V_{MP}}{I_{MP}} \quad (3.5)$$

3.9.2 Series Resistance

Series resistance, R_S in a solar cell has three causes: firstly, the movement of current through the emitter and base of the solar cell; secondly, the contact resistance between the metal contact and the silicon; and finally the resistance of the top and rear metal contacts. The main impact of series resistance is to reduce the fill factor, although excessively high values may also reduce the short-circuit current.

Series resistance does not affect the solar cell at open-circuit voltage since the overall current flow through the solar cell, and therefore through the series resistance is zero. However, near the open-circuit voltage, the IV curve is strongly affected by the series resistance. A straight-forward method of estimating the series resistance from a solar cell is to find the slope of the IV curve at the open-circuit voltage point. Typical values for area-normalized series resistance are between 0.5 Ωcm^2 for laboratory type solar cells and up to 1.3 Ωcm^2 for commercial solar cells.

3.9.3 Shunt Resistance

Significant power losses caused by the presence of a shunt resistance, R_{SH}, are typically due to manufacturing defects, rather than poor solar cell design. Low shunt resistance causes power losses in solar cells by providing an alternate current path for the light-generated current. Such a diversion reduces the amount of current flowing through the solar cell junction and reduces the voltage from the solar cell. The effect of a shunt resistance is particularly severe at low light levels, since there will be less light-generated current. The loss of this current to the shunt therefore has a larger impact. In addition, at lower voltages where the effective resistance of the solar cell is high, the impact of a resistance in parallel is large. An estimate for the value of the shunt resistance of a solar cell can be determined from the slope of the IV curve near the short circuit current point. Typical values for area-normalized shunt resistance are in the MΩ cm^2 range for laboratory type solar cells, and 1000 Ωcm^2 for commercial solar cells.

3.9.4 Effect of Temperature

Like all other semiconductor devices, solar cells are sensitive to temperature. Increases in temperature reduce the band gap of a semiconductor, thereby effecting most of the semiconductor material parameters. Fig 3.9 depicts the effect of temperature on an I-V curve. When a PV cell is exposed to higher temperatures, I_{SC} increases slightly, while V_{OC} decreases more significantly.

For a specified set of ambient conditions, higher temperatures result in a decrease in the maximum power output P_{MAX}. Since the I-V curve will vary according to temperature, it is beneficial to record the conditions under which the I-V sweep was conducted.

3.9.5 Effect of Light Intensity

Changing the light intensity incident on a solar cell changes all solar cell parameters, including the short-circuit current, the open-circuit voltage, the FF, the efficiency and the impact of series and shunt resistances.
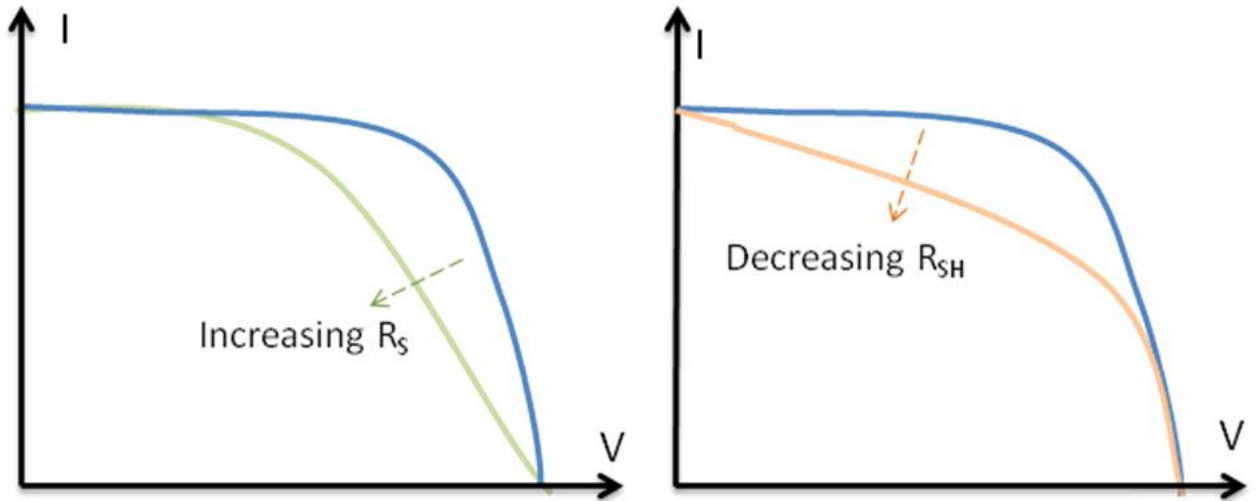
Figure 3.8: Effect of diverging R_s and R_{SH} from ideality
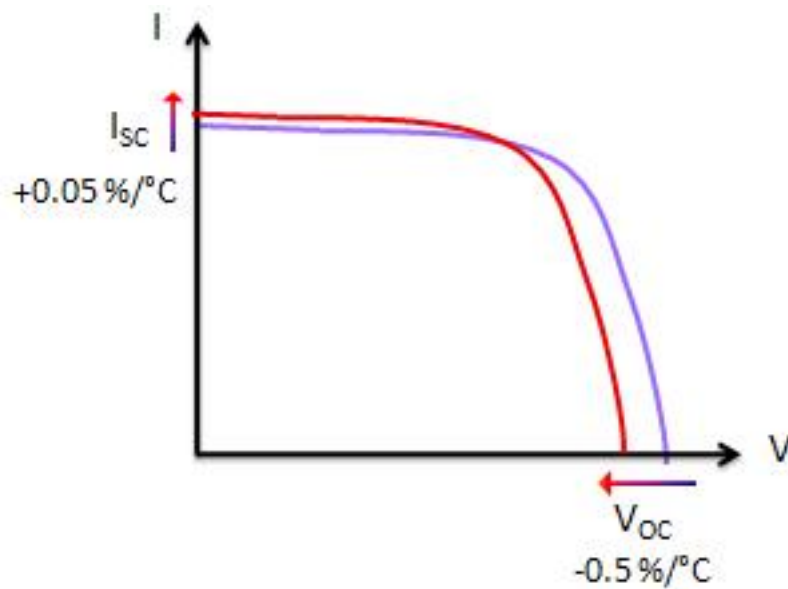
Figure 3.9: Temperature effect on I-V Curve

As the light intensity changes, both current and voltage of solar cell varies. But the variation in the current is much more significant than the variation in the voltage. The IV curve shifts downwards as light intensity decreases as shown in Fig. 3.10

3.9.6 Solar cell model

PV cells can be modeled as a current source in parallel with a diode. When there is no light present to generate any current, the PV cell behaves like a diode. As the intensity of incident light increases, current is generated by the PV cell. In the presence of both series and shunt resistances, the IV curve of the solar cell is given by;
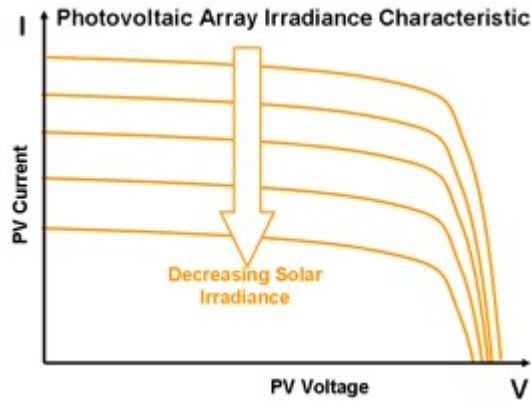
Figure 3.10: PV cell irradiance characteristics

$$I = I_L - I_0 exp\left[\frac{q(V + IR_s)}{nKT}\right] - \frac{V + IR_s}{R_{sh}} \tag{3.6}$$

and the complete model of the solar cell is shown in Fig 3.11.
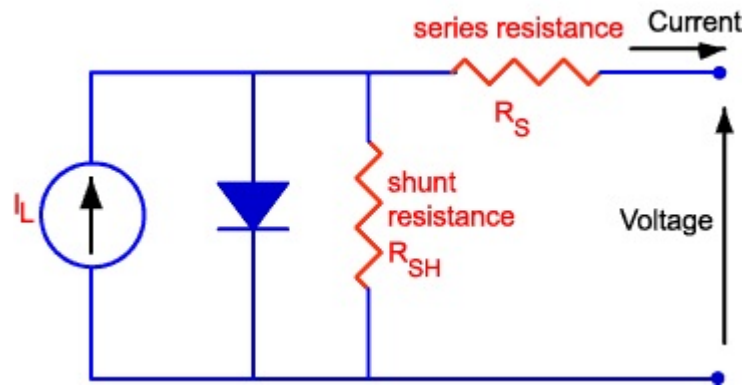
Figure 3.11: Solar cell model

3.10   Conclusions

Among all the environmental energy sources the solar energy has a lot of advantages and is widely available. The power density of solar source is high when compared with the other sources. The power delivered from a solar cell depends on the light intensity and the load connected to it. Power output is zero at zero load impedance (short circuit) and infinite load (open circuit) and maximum power occurs in between these two points. An interfacing circuit (energy harvesting circuit) is needed to ensure solar cell is operating in maximum power region.

Chapter 4

Design of ultra-low power solar energy harvesting system

4.1 Introduction

The Photovoltaic (PV) cells are used to transform solar energy into electrical energy. The output power of PV cells varies with light intensity and temperature [4]. Under a certain light intensity, the PV cell's output power is depending on the load, and the output power reaches the maximum for a certain load value when the PV cells operate at the maximum power point (MPP). In such solar cell power supply systems, it often requires that the maximum power point of the solar array is tracked (MPPT), in spite of the variations in the load and the sunlight intensity, to make the most efficient use of the solar array and the storage battery. For large scale energy harvesting systems, the power used for MPP tracking is negligible when compared to total harvested power. Hence in those systems one can implement complex circuitry or even a separate processor to implement MPP tracking algorithm. But the scenario is entirely different for ultra-low power systems because here the losses in the harvesting system are comparable with the total harvested power. This introduces a lot of new design challenges in the development of MPPT system.

4.2 Concept of MPPT

A power source will deliver its maximum power to a load when the load has the same impedance as the internal impedance of the power source. In solar energy harvesting system, solar cells are the source and rechargeable batteries are the load. In its simplest form of solar harvesting, charging is carried out by connecting the PV array directly across the battery. However the battery itself behaves as power source, therefore the operating voltage of the solar array is equal to the battery voltage. Hence the direct connection cannot provide the optimum operating voltage. For that a voltage regulator is placed to between solar cell and battery to isolate them. This arrangement cannot serve maximum power extraction from solar cell. Therefore a Maximum Power Point Tracking circuit is required to control the voltage regulator.

This requirement can be also visualized through solar I-V characteristic shown in Fig 4.1. From the Fig 4.1 it is clear that the power obtained from the solar cell is zero at open circuit (infinite impedance) and short circuit (zero impedance). So, the operating point of solar cell has to fix at a point (termed as MPP) in between

these two for delivering maximum power to the load.
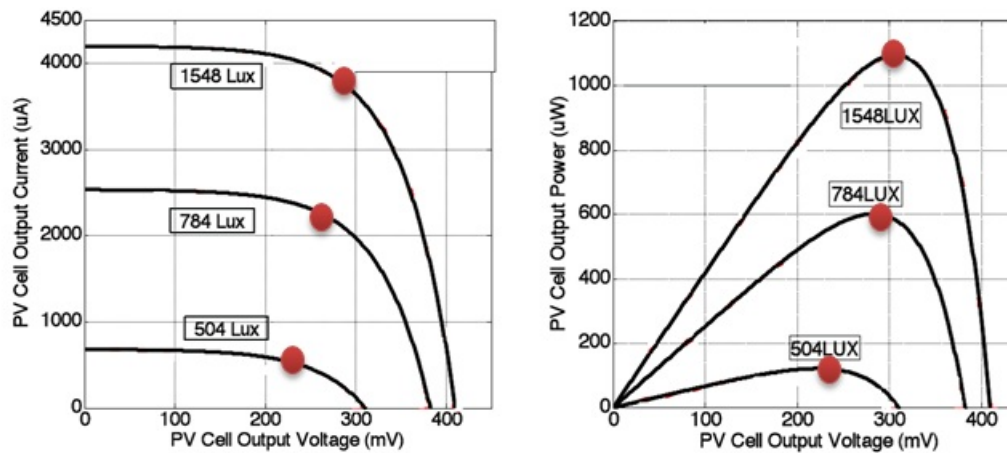
Figure 4.1: I-V curve and P-V curves showing MPP [20]

Further it has been also noticed that, the characteristic of the PV array is constantly changing due to changes in the intensity of the solar light falling on the array as well as to changes in the ambient temperature, as a result the MPP also changes. Therefore the system needs a control unit to track the MPP dynamically. The complete energy harvesting unit is a form of solar cell, voltage regulator (DC-DC converter), control unit and battery as shown in Fig. 4.2. The control unit determines the operating point of the voltage regulator using MPPT algorithms. High performance MPPT modules may incorporate software algorithms to take account of the variations in insolation and temperature.
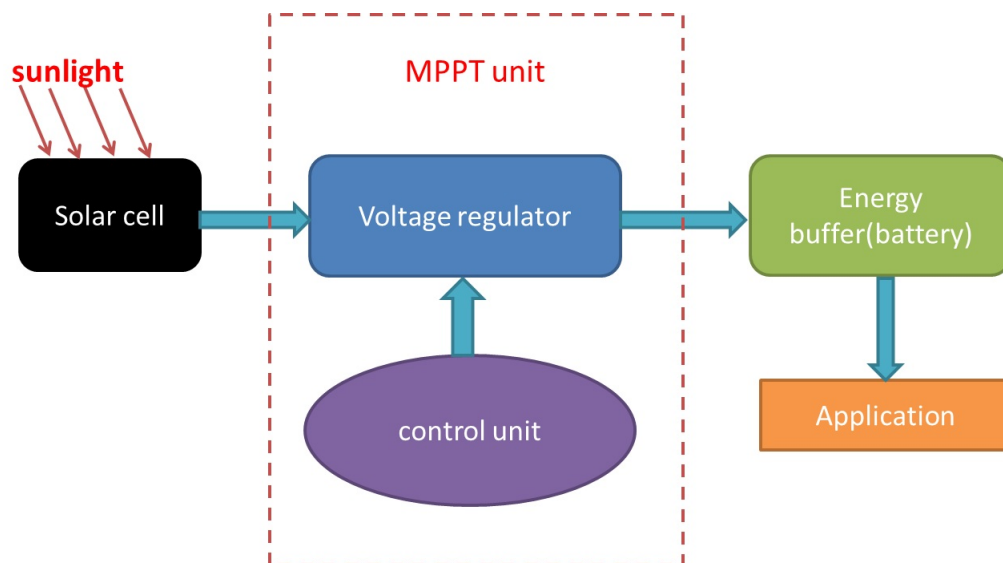
Figure 4.2: Generic MPPT system

In the design of energy harvesting unit, researchers have connected voltage regulator (DC-DC converter) directly to the load (application) without battery interface [5]. In this scheme, the converter input impedance is changed by tuning the converter switching duty cycle and try to match with load impedance. So the out voltage of the DC-DC converter depends on the input voltage and the duty cycle. However, as the solar

cell voltage is varying in real environment that make the variation in the duty cycle (to track MPP) of the converter for matching. But as a result, the output voltage of converter also varies quite amount. Therefore, the unstable converter output cannot be used to power the application (load) directly. So we can conclude that the DC-DC coveter should interface the load through a rechargeable battery instead of direct feeding to load. If any application requires a supply voltage different from the battery voltage, a second DC-DC converter can be used to generate a stable supply from the battery.

4.3   Design challenges for micro scale systems

Scaling down is the modern trend in the electronics industry and all the device dimensions are shrinking. More over the applications of the micro scale devices like wireless sensor networks and implants can work better if their size is reduced. Reduction in the size causes cost reduction also, hence bulk manufacturing of these devices become cheaper. In short, modern ultra-low power devices has a lot of design constrains in terms of area, cost and power. The designer has to take care these constrain in the design. In micro scale systems, stacking of multiple solar cells is not viable due to size and cost constraints. Therefore the recent trend is to use a single solar cell (0-0.5V). However it is very difficult to drive a load using single solar cell due to low output voltage [20]. Scavenging energy from such low voltage sources require judicious circuit design. Moreover the storage batteries normally work on or above 1V, a DC-DC converter is needed to step-up the voltage before storing in a battery. Commercially available DC-DC converters can provide power conversion efficiencies as high as 95% for input voltages much greater than 1V. However, it is difficult to obtain such high efficiencies for ultra-low input voltages, say less than 0.4V [41]. Therefore the major design challenge is to design an efficient DC-DC converter. In various literatures, charge pump based converter has been preferred over Inductor based one due to fully on chip integration.

In the charge pump based MPPT system, the frequency of the charge pump is adjusted to vary the impedance so that it matches with the solar impedance. If the frequency of the charge pump is increased from zero to infinity the power/current obtained from solar cell increases, reaches a maximum (at knee frequency) and then saturates as shown in the Fig.4.3. But as the frequency increases the losses inside the charge pump goes on increasing almost linearly [20]. Since the power obtained from micro scale solar cell system is very less (in micro watt range), the power loss in the DC-DC converter (charge pump) and the MPPT control unit is comparable to the total harvested power. Therefore the total power harvested is the difference between the two.

$$P_{out} = P_{solar} - P_{Loss} \tag{4.1}$$

In general, for getting maximum power, the losses in the circuit should be minimum. Losses in charge pump become less at the low clock frequency. But at low frequency, the harvested power also becomes less. Therefore, Fig 4.3 suggest that the clock frequency should be select such a way , that at that frequency (P_{solar}-P_{loss}) become maximum and this point is the system MPP. Therefore just maximizing the solar output power will not give the system MPP. Effectively the solar MPP and the system (solar + charge pump) MPP may be different. It is illustrated in Fig. 4.4. Recently, Lu.et al also verified it experimentally for micro scale systems [23].
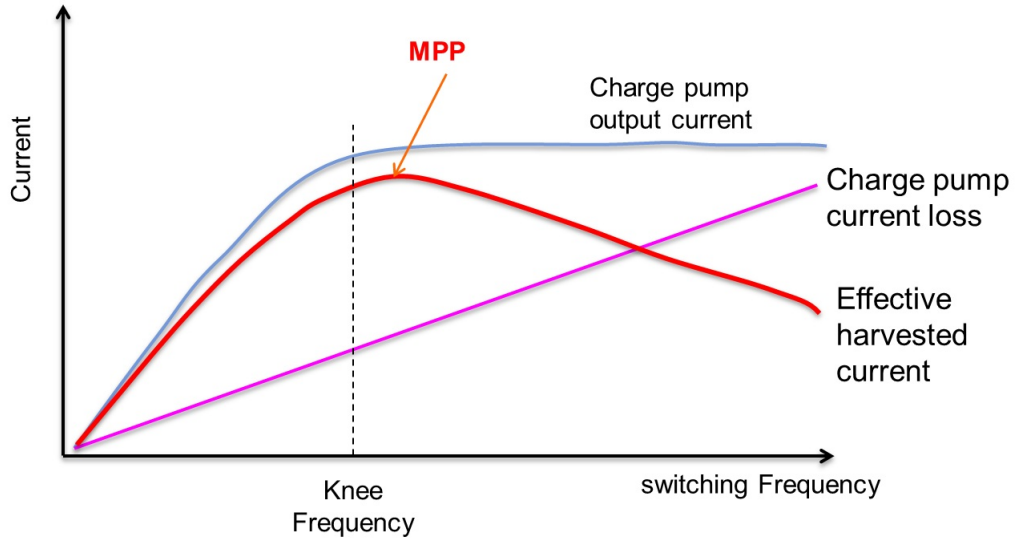
Figure 4.3: Current frequency relationship of charge pump
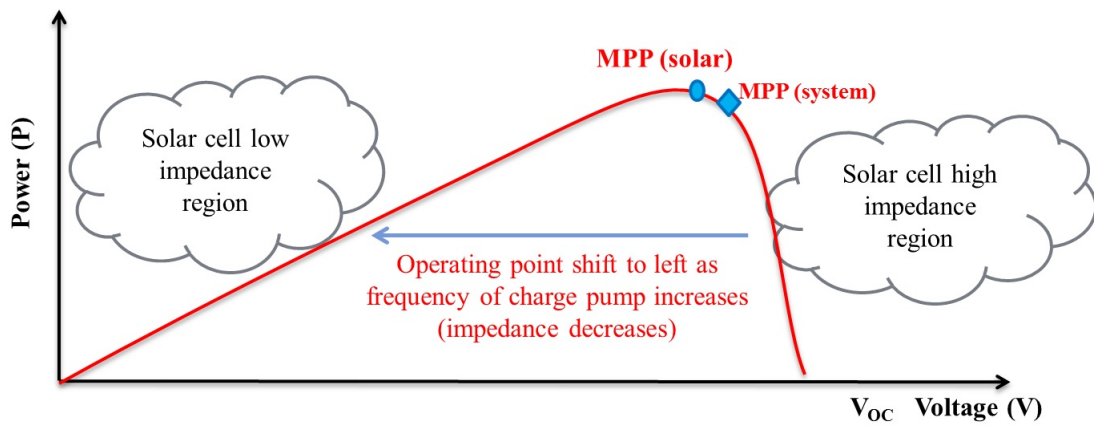
Figure 4.4: Voltage-power characteristics of solar cell

4.4 Solar energy harvesting system

4.4.1 Introduction

Solar energy harvesting system converts solar energy to electrical energy in an efficient way and stores the energy. A typical solar energy harvesting system consists of solar cells, a DC-DC converter (charge pump for on chip integration), control unit and an energy buffer (battery). The solar cell converts light energy to electrical energy. The charge pump is used to step up the DC voltage to the required level, and the battery to store the electrical energy. The control unit performs the MPPT by providing optimum frequency to the charge pump so that its impedance is matched to the solar cell impedance dynamically.

There are two major design challenges for proper MPP tracking system such as (i) Efficient DC-DC converter and (ii) MPPT algorithm.

26

4.4.2 MPPT methods

Numerous researchers [14-19] have designed MPPT for micro scale solar energy harvesting.

4.4.3 Design time component matching

Heliomote [14] is one of the first wireless sensor nodes that used solar energy harvesting for power. But in this sensor node MPP tracking is absent. Near MPP operation is ensured by careful selection of the components. This method is called design time component matching (DTCM). The solar panel is connected to a battery whose terminal voltage determines the panel's operating point along its V-I curve. They ensured operation at the maximal power point while avoiding the use (and overhead) of an MPPT circuit through the choice of battery. Using two NiMH batteries to operate the Heliomote, the battery voltage varies between 2.2V and 2.8V, which, together with a diode used to prevent reverse current flow into the solar panel, ensures that the voltage across the solar panel terminals remains close to optimal (MPP of their PV cell varies between 2.5-3.0 V). In addition, by avoiding the use of a Li+ battery, their charging circuit is considerably simplified, leading to increased efficiency. The AA size also retains compatibility with the mote form factor and enables reuse of the mote's original battery case, thereby reducing cost.

Figure 4.5: Heliomote a solar harvesting sensor node

Since operating point PV cell is fixed by the battery, this technique fails to track MPP. Moreover this method cannot be used for low voltage applications (eg: single solar cell) as the single PV cell output voltage is low ($\sim$0.4V).

4.4.4 Fractional open circuit voltage method

One of the simplest MPPT methods is the fractional open circuit voltage (FOCV), which exploits the nearly linear relationship between the PV panel open-circuit voltage (V_{OC}) and its voltage at the MPP (V_{MPP}) under varying irradiance and temperature levels. Therefore to get the V_{MPP}, the load is disconnected from the

PV cells and the open circuit voltage is measured. MPP voltage is derived from open circuit voltage using following relation. $V_{MPP}= \alpha \, V_{OC}$ Here α depends on the PV module used. However, this result is based on observations and must be empirically determined for each specific type of PV panel. [42].

Table 4.1: FOVC method relation between V_{OC} and V_{MPP} (from [18])

V_{OC} (V)	V_{MPP} (V)	α
3.24	2.50	0.772
3.40	2.52	0.741
3.40	2.44	0.717
3.60	2.80	0.778
3.60	2.60	0.722
3.96	2.92	0.737
4.50	3.50	0.778
4.50	3.30	0.733

The disadvantage of this method is that frequently disconnecting PV cells from the load causes power loss and requires circuit for time multiplexing. An improved design was proposed by D. Brunelli & L. Benini [18] which eliminates the power loss due to frequent disconnecting the PV cell from load by adding a tiny PV cell. This tiny PV cell is used to calculate the V_{MPP}. However this method is not cost effective as two cell is required for its operation.

4.4.5 Hill climbing/ perturb and observe algorithm

Hill climbing / perturb and observe methods are suitable for MPP tracking, when partial shading is not considerable [43]. This method involves applying a small perturbation in the operating point of the power converter and the output is compared with the previous output. The comparison result is used to determine the direction of the next perturbation. If the perturbation results in power increase, next perturbation is applied in the same direction. If the perturbation results in power decrease, next perturbation is applied in the opposite direction of the previous. This process repeats until MPP is reached. In steady state, the system oscillates around the MPP. This is a closed loop method and it gives system MPP. The algorithm is given in a tabular form in Table 4.2.
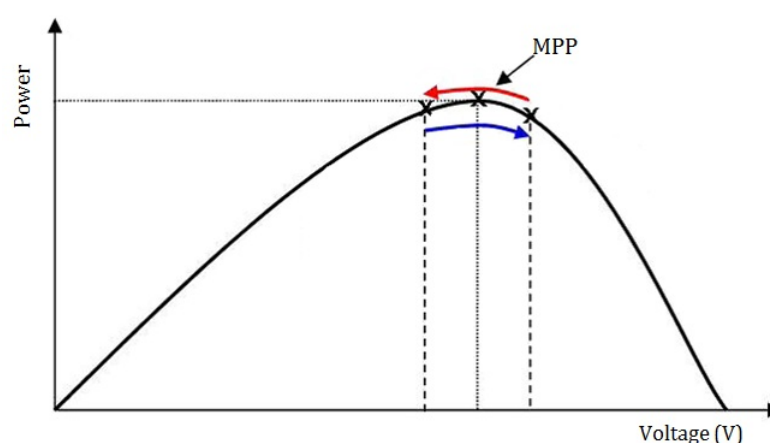
Figure 4.6: Characteristic PV array power curve

28

Table 4.2: Perturb and observe algorithm

Perturbation	Change in power	Next perturbation
Positive	Positive	Positive
Positive	Negative	Negative
Negative	Positive	Negative
Negative	Negative	Positive

4.5 Conclusions

In a solar energy harvesting system maximum power is delivered to load only if the impedances solar cell and load are matched. Hence simply connecting solar cell to battery or load will not provide efficient energy harvesting and we need an MPPT circuit to dynamically adjust the load with solar impedance as light intensity is varying. Micro scale energy harvesting faces lot of challenges since the harvested power is very less. Hence the selection of MPPT algorithm and charge pump circuit is very crucial for efficient energy harvesting.

Chapter 5

Charge pump

5.1 Introduction

Charge pumps are electronic circuits that produce an output voltage several times higher than the input voltage [25, 44]. Charge pump circuits are used for obtaining higher voltages than normal power supply voltage in flash memories, DRAMs and low voltage designs [45]. Charge pump uses only switches and capacitors and hence require very less area compared to other DC-DC converters like buck, boost etc [19]. The switches in the charge pumps are implemented using MOSFETs and hence it is very compatible with modern CMOS technology.

5.2 Working principle

The working of the charge pump is similar to that of a voltage doubler and a simplified diagram of a two stage charge pump is shown in Fig. 5.1.
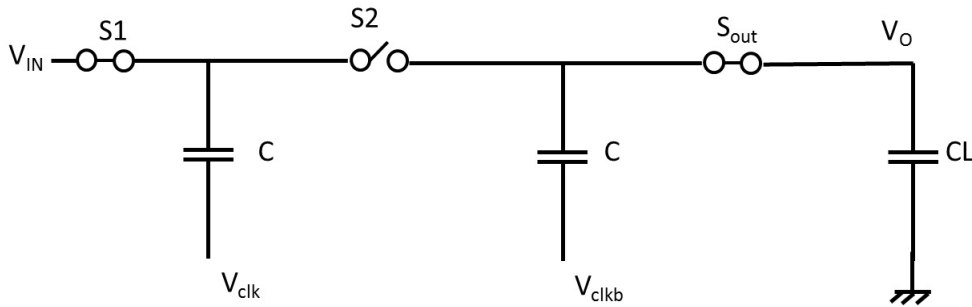
Figure 5.1: Two stage charge pump

Basically, the voltage multiplication is happened in a charge pump by charge sharing mechanism in the capacitors through MOSFET switches. A clock signal (V_{clk} , V_{clkb}) is applied for turning ON and OFF of the MOS switch. During the first half clock period, V_{clk} goes LOW and as a result only the odd switches are closed. So, the first pumping capacitor is charged to V_{IN} and all the other pumping capacitors in the odd stages receive the charge from the capacitor of the previous stage as shown in Fig 5.2.
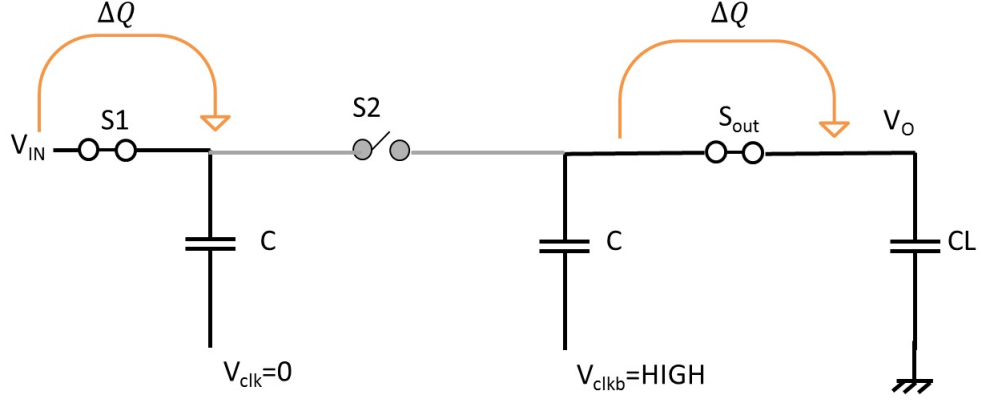
Figure 5.2: Charge sharing in first half cycle

During the subsequent half clock period, the signal V_{clk} goes to HIGH and turns on only the even switches. As a result, all the capacitors in the odd stages give the charge to the capacitor in the subsequent stage.
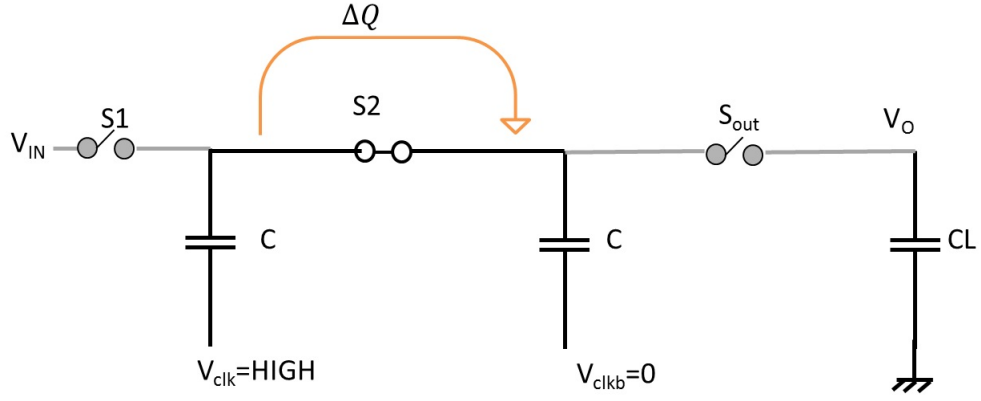
Figure 5.3: charge sharing in second half cycle

So as a conclusion, in a complete clock period, each charge pump capacitor receives an amount of charge from the capacitor at its left side and gives a part of this charge to the capacitor at its right side. Thus, in each period there is a charge transfer from the input to the output load. At each cycle the voltage of the load capacitor will increases and finally reaches to asymptotic value. Several cycles are needed to approach the asymptotic to the final value as shown in Fig. 5.4. The step increment of the output voltage in each successive clock period becomes very less compared to final value.

Thus, a charge pump takes charges from the input via the capacitor C, pumps these charges into the output load and, the voltage of output capacitor increases up to a stable value that is several times of the input voltage, depending on the number of stages.

5.3   Low power architectures

Charge pump was first proposed by Dickson [46] and it had a linear topology. But it is not suitable for low voltage operation, as switches are form of diode based in this configuration and that causes extra voltage

Figure 5.4: Output voltage of charge pump (from [25])

drop (diode ON voltage) in each stage. Therefore, number of literatures has been emphasized on low-voltage charge pump design w.r.t different application. Since our work has been focused on solar cell applications, we have noticed the following design challenges for low-voltage charge pump:
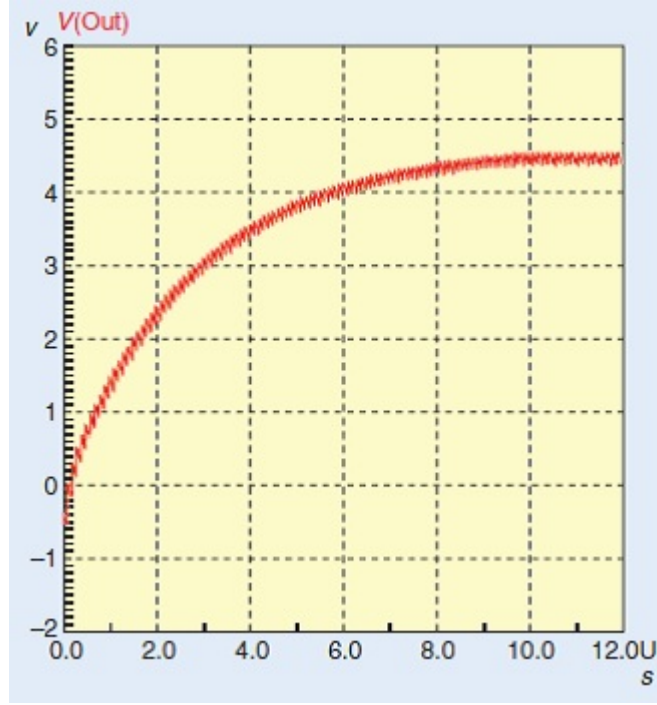
- Complete charge transfer in each stage of charge pump is difficult to achieve as the input voltage is very low.

- Due to body effect, the threshold voltage of MOSFET increases as number of stage increases (body is grounded and source voltage increases in each stage).

- The power obtained from the source is very less. So the power dissipation of the charge pump should be very less.

- Since the input voltage is very low, the ON resistance of MOS switches is very important and it should be minimum.

To counteract with the above design challenges, the control strategy of linear charge pump have been extensively studied and optimized [47, 26]. However, the optimized linear charge pump topologies performance degrades substantially in an ultra-low voltage (sub threshold) energy transducer. As, the charge transfer capability and the efficiency of the charge pump reduce drastically if the input voltage is comparable to threshold voltage of MOSFET (the output voltage of a solar cell is about 0.5V or below).

In order to improve the power conversion efficiency, cross-coupled charge pumps have also been proposed [48, 49]. However, this topology also fails to function normally in very low voltage. In [50], an exponential topology charge pump was proposed to extract energy from ultra-low voltage sources. However, the charge transfer capability of this topology is still impeded by the first stage. Recently, Lu.et al [20] proposed a tree

topology charge pump for boosting ultra-low input voltages. They have shown that their design improved charge transfer capability by up to 30% as compared to linear topology charge pumps. In our work, we have incorporated this topology for our proposed solar energy harvesting system

5.3.1 Linear charge pump

A linear charge pump has a linear relationship between output current and switching frequency. The circuit diagram of an optimized 3-stage 4× linear charge pump with step up ratio of 4 (ideal case) is shown in Fig. 5.5.
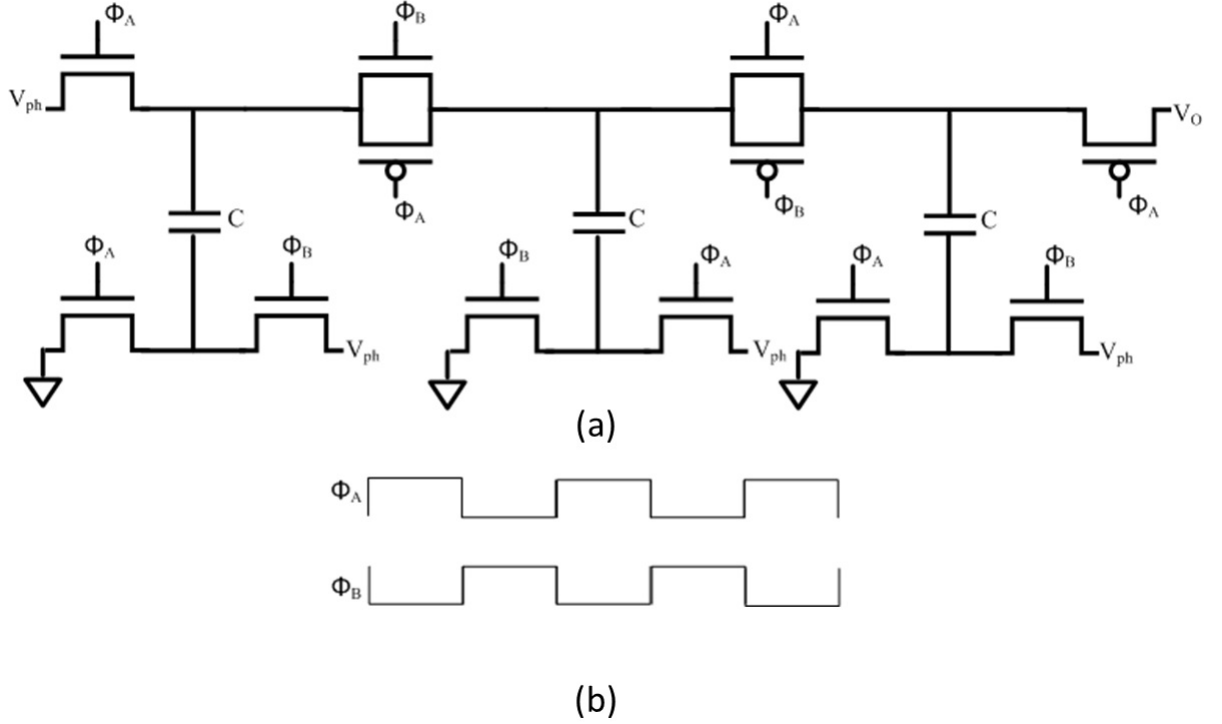
Figure 5.5: 3 stage linear charge pump

Through a mathematical analysis described in [19, 26], the average output current from a 3-stage linear charge pump can be expressed as

$$I_{out} = \frac{1}{3}CF_{clk}(4V_{ph} - V_o) \tag{5.1}$$

The above equation is derived based on the assumption that complete charge sharing is guaranteed within each clock cycle. It reveals a linear relationship between the charge pump output current (I_{out}) and switching frequency(F_{clk}), when the capacitor (C), scavenger voltage (V_{ph}) and energy buffer voltage (V_o) are constant. Practically, it has been observed the above linear relationship holds with low clock frequency (as shown Fig 5.6). As the frequency increases beyond a certain value, the charge sharing becomes incomplete. Hence, the linear relationship between output current and switching frequency does not hold beyond the knee frequency and the output current is saturated.

Figure 5.6: Charge pump output current vs the applied switching frequency

5.3.2 Tree topology charge pump

Tree topology charge pump may be more suitable for single solar harvesting operation, as it has shown a good performance compared to linear topology in ultra low voltage [20]. The working of this charge pump is well explained in [20] and the current equation (Eq. 5.2) is given by

$$I_{out} = \frac{1}{N}CF_{clk}[(N+1)V_{ph} - V_o] \tag{5.2}$$

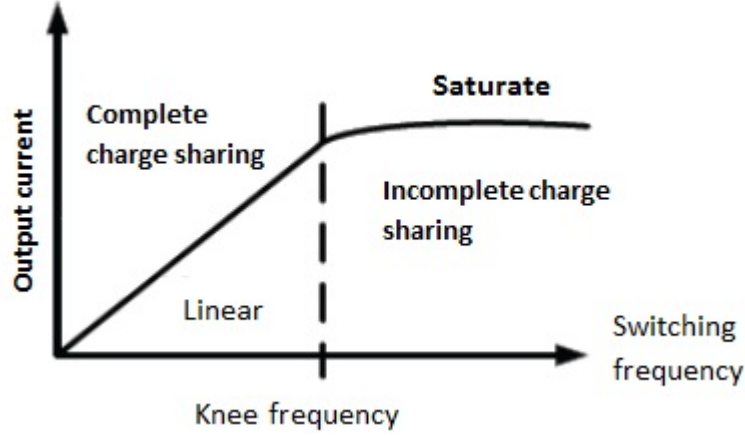The front-end stages (Fig 5.7) operate like voltage doublers. The back end stage boosts the front-end output voltage further to a higher voltage. This structure has the same hardware cost (i.e., 12 MOS transistors and 3 capacitors), as 3 stages 4× linear topology (Fig. 5.5). However, the tree topology structure provides better performance as it has a higher knee frequency (as shown in Fig. 5.8), that helps it to operate in higher frequency compare to linear topology. In our design, we have used the tree topology structure and the losses of the charge pump has been described in following section to evaluate the performance of solar energy harvester.

5.4 Loss analysis

5.4.1 Introduction

In micro scale energy harvesting systems, the harvested power is very less and is comparable to the losses in the circuit. Hence minimizing the losses are as important as harvesting energy. More over the maximum power point not only depend on solar cell but also on the charge pump. In some MPPT circuit design, prior characterization of the charge pump is needed. Hence the loss analysis is very relevant in micro scale systems. The block diagram of a typical solar energy harvesting system is shown in Fig. 5.9. Majority of the losses occur in the charge pump. The losses occurring during power transfer is analyzed and modeled in [51]. It includes switching power loss, conduction power loss and leakage power loss. This section explores the losses and their effect to determine the system performance.

Figure 5.7: Tree topology charge pump

Figure 5.8: Knee frequency comparison between two topologies

5.4.2 Conduction Power Loss

In the CMOS based charge pump, MOSFETs based switches are used, they work in cutoff region in OFF state and in linear region in ON state. Since, in ON condition, MOSFET has a finite on-resistance that causes a conduction power loss in the charge pump. That can be modeled with the ON- resistance of a MOSFET
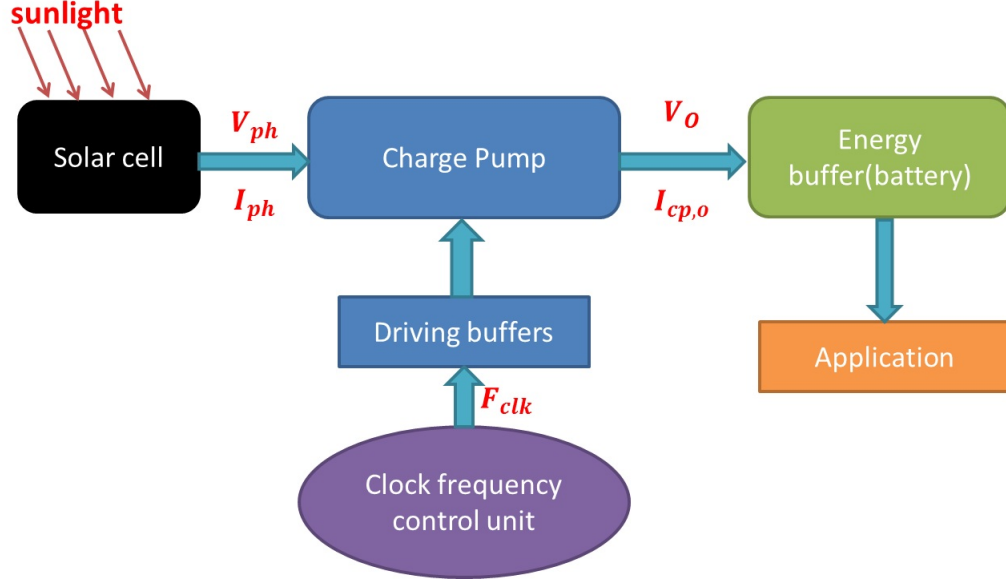
Figure 5.9: Typical energy harvesting system

given as

$$R_{on} = \frac{1}{\mu C_{ox}\left(\frac{w}{l}\right)\left(V_{gs} - V_{th} - \frac{1}{2}V_{ds}\right)} \tag{5.3}$$

Then the power loss due to ON- resistance,

$$P_{con} = \frac{I_{on}^2}{\mu C_{ox}\left(\frac{w}{l}\right)\left(V_{gs} - V_{th} - \frac{1}{2}V_{ds}\right)} \tag{5.4}$$

As, in a charge pump, MOSFET is turned ON for half of the clock cycle. Hence the average power loss is given by

$$P_{con\_avg} = \frac{1}{2}M\frac{I_{on}^2}{\mu C_{ox}\left(\frac{w}{l}\right)\left(V_{gs} - V_{th} - \frac{1}{2}V_{ds}\right)} \tag{5.5}$$

Where M is the total number of MOSFET switches in the circuit. This equation shows that conduction power loss is inversely proportional to the width (W) of the MOSFET switch. So by increasing the W, we can reduce the loss.

5.4.3   Switching Power Loss

Moreover, the turn ON and OFF of MOSFETs switching contributes another power loss, termed as switching loss. This loss occurs due to the charging and discharging of MOSFET gate capacitance during switching. Usually the sizes of the MOSFETs in the switches are huge to reduce the ON resistance. Hence a buffer is used to drive the switches (shown in Fig. 5.10) because clock signal can't drive them directly. The driving buffers consist of inverter chain with increasing the size.

In this driver circuit, each stage drives an inverter with a size of three times higher than previous one. The switching power loss of a power MOSFET with gate capacitance C_g is given as
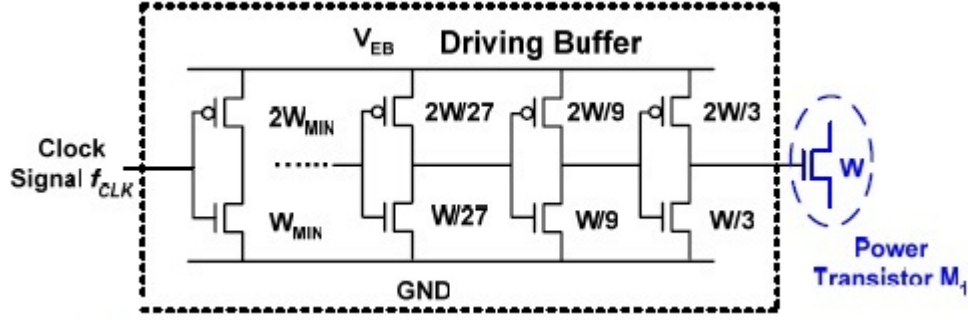
36

Figure 5.10: Schematic view of driving buffer and a power MOSFET

$$\mathrm{P}_{swt} = C_g V_o{}^2 F_{clk} \tag{5.6}$$

If C_{ox} is the capacitance per unit area, then

$$\mathrm{P}_{swt} = C_{ox}(Wl)\, V_o{}^2 F_{clk} \tag{5.7}$$

Since, the size ratio of successive stages in the driving buffer is three and in the same stage, a PMOS transistor is twice the size of a NMOS transistor, thus, the switching power loss due to PMOS transistors in a driving buffer is estimated as:

$$\mathrm{P}_{swt} = C_{ox} l V_o{}^2 F_{clk} \sum \left(\frac{2W}{3} + \frac{2W}{9} + \frac{2W}{27} + ... \right) \tag{5.8}$$

After simplification of Eq 5.8 , the switch loss due to PMOS part,

$$\mathrm{P}_{swt\_p} = C_{ox}(Wl)\, V_o{}^2 F_{clk} \tag{5.9}$$

Similarly, the switching power loss in the NMOS part is given as

$$\mathrm{P}_{swt\_n} = \frac{1}{2} C_{ox}(Wl)\, V_o^2 F_{clk} \tag{5.10}$$

The total power loss is the sum of loss due to power MOSFETs and the driver MOSFETs and it is given by,

$$\mathrm{P}_{swt\_total} = M \left(P_{swt\_p} + P_{swt\_n} + P_{swt\_M} \right) \tag{5.11}$$

hence,

$$\mathrm{P}_{swt\_total} = \frac{5}{2} M C_{ox}(Wl)\, V_o^2 F_{clk} \tag{5.12}$$

Where M is the total number of power MOSFETs in the charge pump, W and l are the width and the length of MOSFETs. F_{clk} is the clock frequency of the charge pump. V_O is the battery voltage. The Eq 5.12 says that the switching power loss is directly proportional to width of the MOSFET and suggest that to reduce the power loss, W should be minimum.

5.4.4 Leakage Power Loss

Leakage power loss is mainly due to the weak conduction of transistors when they are turned off. Since the drain leakage current varies exponentially with its gate control voltage, the ratio of I_{ON}/I_{OFF} is about 10^3 in nano scale silicon processes [52]. As a result, leakage power loss is relatively small, compared with other power loss components. In addition of above losses, there is a bias loss, it occurs in all the module of complete system, expressed as

$$P_{bias} = I_{bias}V_{bias} \tag{5.13}$$

5.5 Tuning of MOSFET sizes for optimum performance

There is multiple charge sharing paths in series or parallel depending on the configuration of a charge pump as shown in Fig 5.11. The ON resistance of the MOSFETs varies from one charge sharing path to another path. This happens because ON resistance depends on the voltage across the MOSFET and the voltage level is different for different charge sharing paths. The expression for ON resistance is given below.

$$R_{on} = \frac{1}{\mu C_{ox}\left(\frac{w}{l}\right)\left(V_{gs} - V_{th} - \frac{1}{2}V_{ds}\right)} = \frac{1}{\mu C_{ox}\left(\frac{w}{l}\right)\left(V_g - V_{th} - \frac{1}{2}(V_d + V_s)\right)} \tag{5.14}$$

Eq.5.14 reveals that the conduction resistance Ron diminishes with the decrease of VS+VD. There are three charge sharing paths inside the 3-stage tree topology charge pump. The $V_S + V_D$ is not same for all paths as shown in Table 5.1
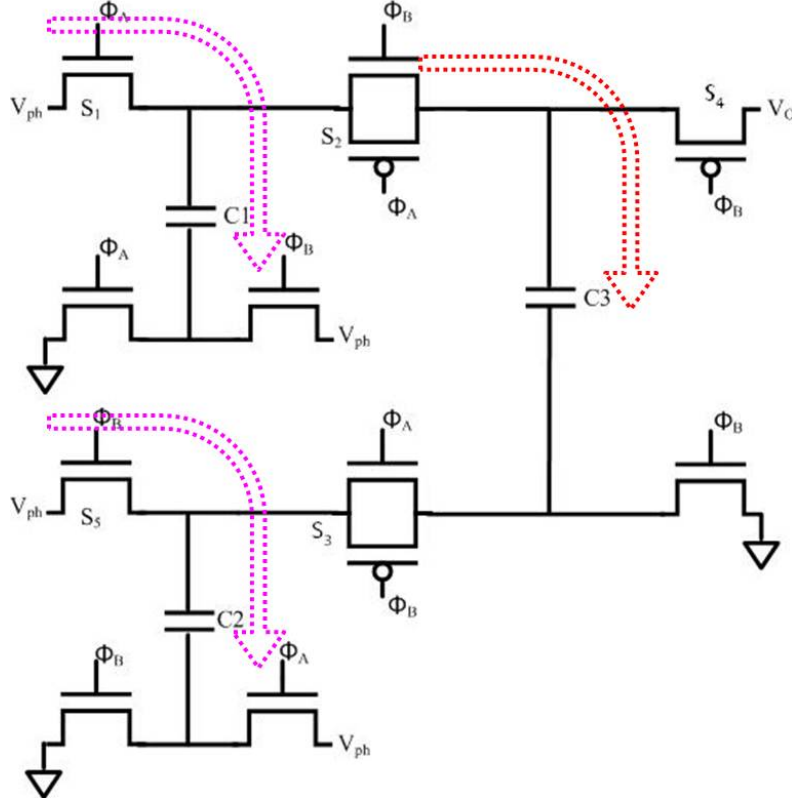

Figure 5.11: Tree topology charge pump showing charge sharing paths

Table 5.1: Drain and source voltages of tree charge pump before charge sharing [20]

Charge sharing path	V_S	V_D	$V_S + V_D$
S_1 and C_1	V_{ph}	V_O-$3V_{ph}$	V_O-$2V_{ph}$
S_5 and C_2	V_{ph}	V_O-$3V_{ph}$	V_O-$2V_{ph}$
S_2 and C_3	$2V_{ph}$	V_O-$2V_{ph}$	V_O

From Eq. 5.14, it is clear that the ON resistance for the first stages (S_1-C_1 and S_5 - C_2) is less compare to the successive stages (S_2 -C_3). Therefore, conventional uniform MOSFET sizing [20, 25] will cause unwanted switching power loss. So, we can propose that optimizing the size of MOSFETs in individual stages will the help to reduce switching power loss.

5.6 Simulation results and discussion

The charge pump circuit is designed in 0.18 μm CMOS technology and simulated using Cadence Spectre simulator. Initially the widths of the MOSFETs are collectively optimized for effective power transfer and for this particular design, it is found to be 700μm. Then further tuning is carried out by varying the MOSFET size in the first stages. The result is tabulated in Table 5.2

Table 5.2: Effective power gain due to tuning of MOSFET (S_1 and S_5) size with keeping other MOSFETs size W=700 μm

MOS size ((S_1 and S_5)μm)	harvested power (μW)	Switching loss (μW)	Effective harvested power (μm)
260	546.1	71.8	474.3
300	551.5	74.3	477.2
340	555.4	76.78	478.62
380	558.4	72.28	479.12
420	560.7	81.77	478.93
460	562.8	84.28	478.52
500	564.1	86.74	477.36
540	565.3	89.23	476.7
700	577.5	99.12	468.38

As we increase the width of the MOSFET in the first stage, the conduction current increase that cause increment in the harvested power. However the switching current loss increases faster than the conduction current, also it is found that the conduction current saturates beyond a particular size of S_1 and S_5. Hence the effective harvested power decreases after certain width of S_1 and S_5. In this design, the effective harvested power is 468.38μW for a uniform MOSFET width of 700μm but an optimized width (for S_1 and S_5) around 380μm, it is 479.12 μW. Thus, this method gives an additional power gain of 10- 20μW.Tuning of MOSFET sizes for power efficient performance is verified through simulation.

5.7 Conclusion

The power converter (charge pump) plays an important role in the energy harvesting system and design of charge pump for low voltage is challenging. To harvest maximum power the losses inside the circuit should be minimized. The switching power loss increases with MOSFET size and conduction current loss decreases

with MOSFET size. Hence there is an optimum value for the MOS size for minimal power loss. These issues should be taken care while designing the charge pump circuit.

Chapter 6

Design and Implementation of hill climbing algorithm

6.1   Introduction

Hill climbing method is one of the most widely used MPPT algorithm. Accurate implementation of hill climbing algorithm needs DSP processor or micro controllers because of the complexity in the algorithm [10]. In low power systems, we can't afford a micro controller or DSP processor because of the power constrains. Shao.et al [19] implemented Hill climbing algorithm using dedicated hardware to suite low power applications. The system consist of solar array, charge pump, current sensor and a decision making circuit. Their system works for a 3V battery and operates up to a current of 180μA. In our work, a single solar cell is used for area constraint and we have chosen a battery with 1 V to make the system cheep. Under this circumstance, the system implementation faces many difficulties.

Ideally the algorithm will work well for single solar cell system because of the absence of local maxima. But for a single cell system since the output voltage is very less (less than 0.5V), the system have to provide high output current to drive load (400-500μW) . To transfer such high current (500μA) the switching frequency of the charge pump should be high. Same time the current sensor also has to work in high frequency. In this work, we tried to implement the hill-climbing based single solar cell harvesting system using UMC 180nm technology. We have found that the circuit fails to work correctly, due to limitation on current sensor operation and that also is verified through simulation in this chapter.

6.2   Circuit implementation

The block diagram of the implementation of hill climbing algorithm is shown in Fig. 6.1. It consists of a solar cell, charge pump, clock control unit, a current sensor and an optimal power tracking circuit. The charge pump steps up the voltage from the solar cell. MPPT unit monitors the charge pump output power using current sensor and determines the adjustment of the system operating parameter. Based on the adjustment decision, the operating frequency of the charge pump is tuned in order to maximize the system power output. Rechargeable battery is used to support the system continuous operation even when the light source is out.

The MPPT circuit consists of a current sensor, a comparison block and a decision making block. The
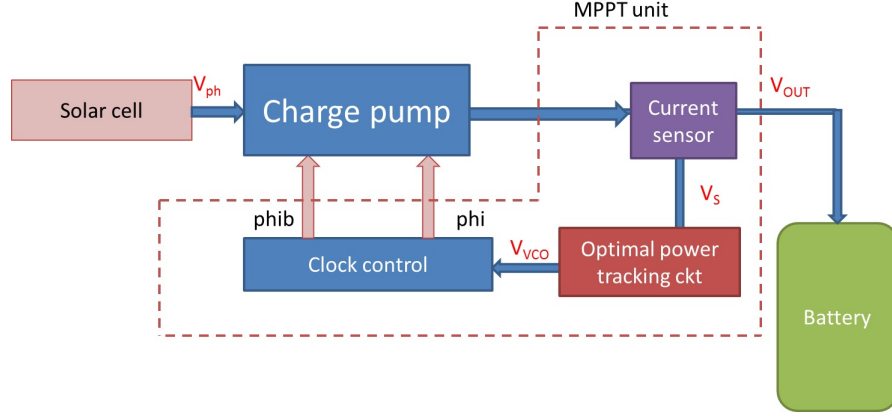
Figure 6.1: Hill climbing method implementation

output of charge pump is connected to the current sensor. The harvested current from the solar cell flows to the battery through the current sensor. The current sensor is used to measure the output current of the charge pump. Since the output voltage of charge pump is almost fixed, maximizing the output power means maximizing the output current.

The operation of a current sensor is similar to a current mirror; this is directly interfaced with charge pump and the circuit diagram of it is shown in Fig.6.2. In current sensor circuit, the size of MOSFET M_1 is very large than M_2 and their ratio is N: 1, as a result a very small proportion of the total output current is diverted to resistor and maximum amount flows to the battery. The current flowing through the resistor produces a voltage (V_S). The comparison block checks this voltage (V_S) to identify the increase or decrease in output current. This information is passed to the control circuit. A smoothing capacitor C_2 is added at the input of the current senor to reduce the pulsating nature of the output current of the charge pump.
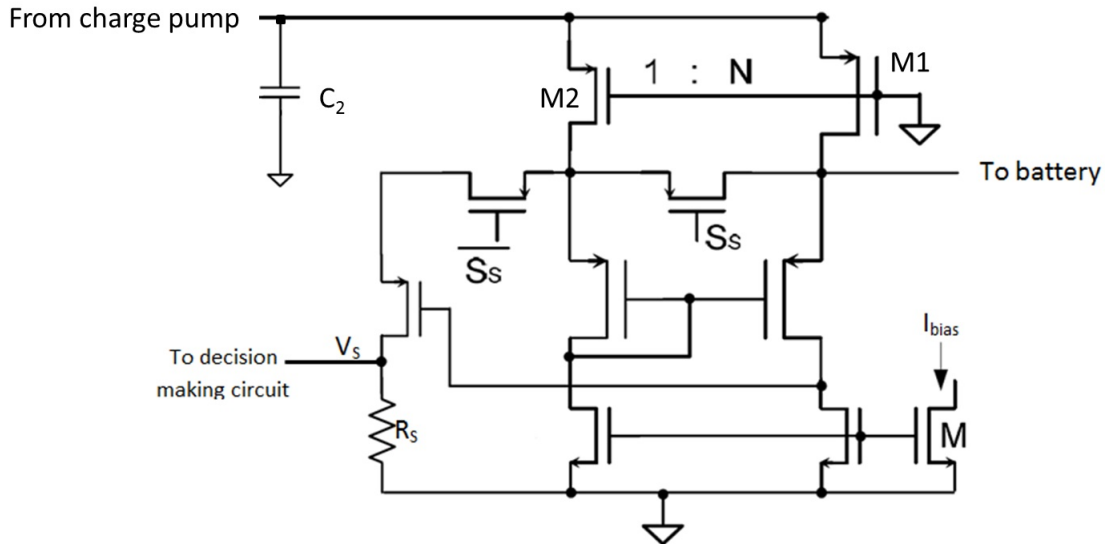

Figure 6.2: Current sensor

The decision making circuit consists of a comparator, D-Flip Flop and XNOR gate. The comparison circuit charges capacitors C_{P1} and C_{P2} alternately using a transmission gate, with respect to control signal
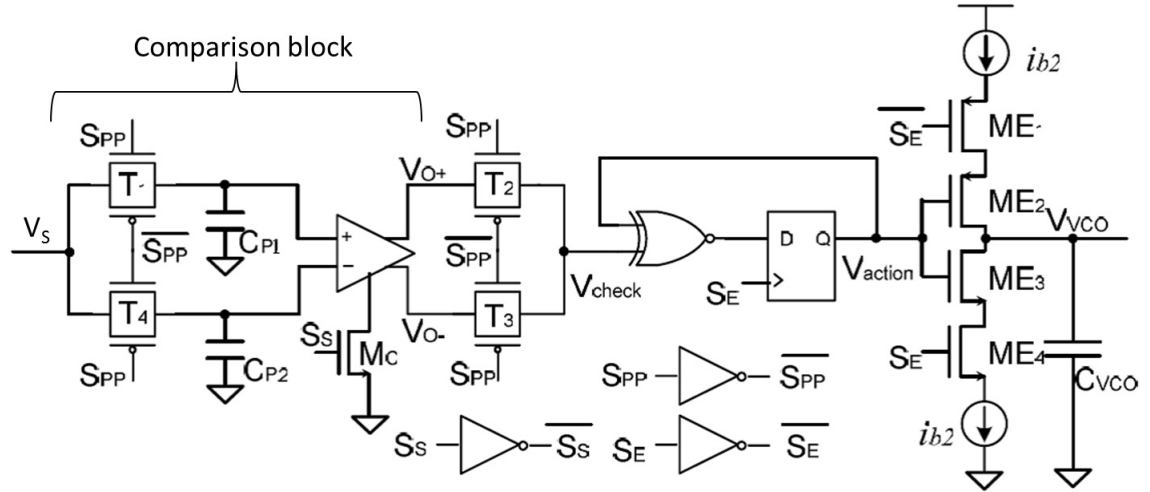
42

Figure 6.3: Decision generation circuit

S_{PP}. A comparator [53] is used to compare the voltage of present sample with previous sample that are stored across C_{P1} and C_{P2}. A control signal S_S is used to enable comparator at the end portion of each S_{PP} half cycle. The waveforms of control signals (S_{PP}, S_S ,S_E) are shown in Fig. 6.4. Signal S_E is used as the clock to the flip-flop.
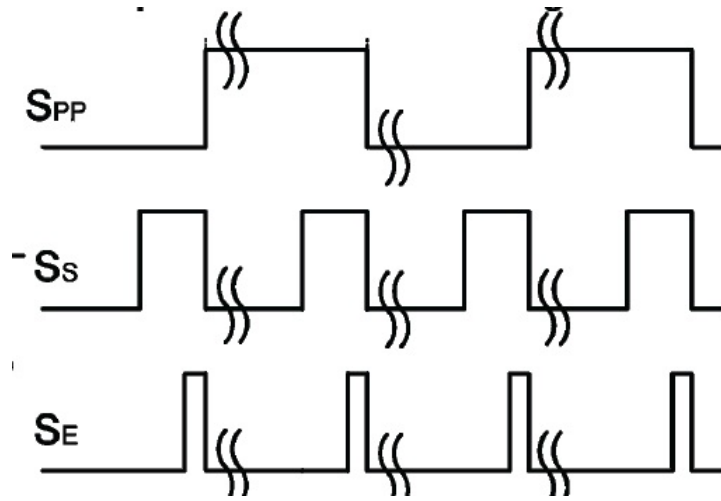
Figure 6.4: Control signals

The comparator output voltage (V_{check}) is XNOR with the previous decision signal, that stored in D flip flop. On basis of that , the decision value V_{action} is updated at the end of clock signal S_E. The logic of V_{action} indicates whether to decrease or increase the charge pump switching frequency. Based on V_{action} value, the capacitor C_{VCO} is either charged or discharged during the control pulse interval of S_E. In this way the voltage V_{VCO} is either increased or decreased and is then sent to the control unit that contains a VCO to adjust the switching frequency of charge pump.

Adding all the modules, we have tried to verify the operation of hill-climbing unit for single solar cell regime in CADENCE.

Figure 6.5: Control unit for the charge pump
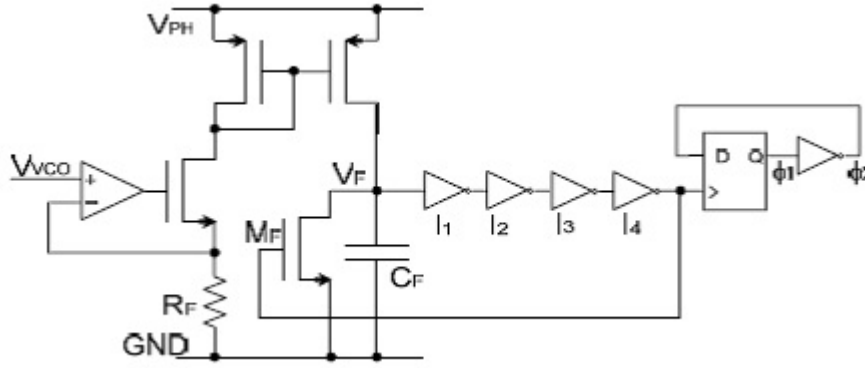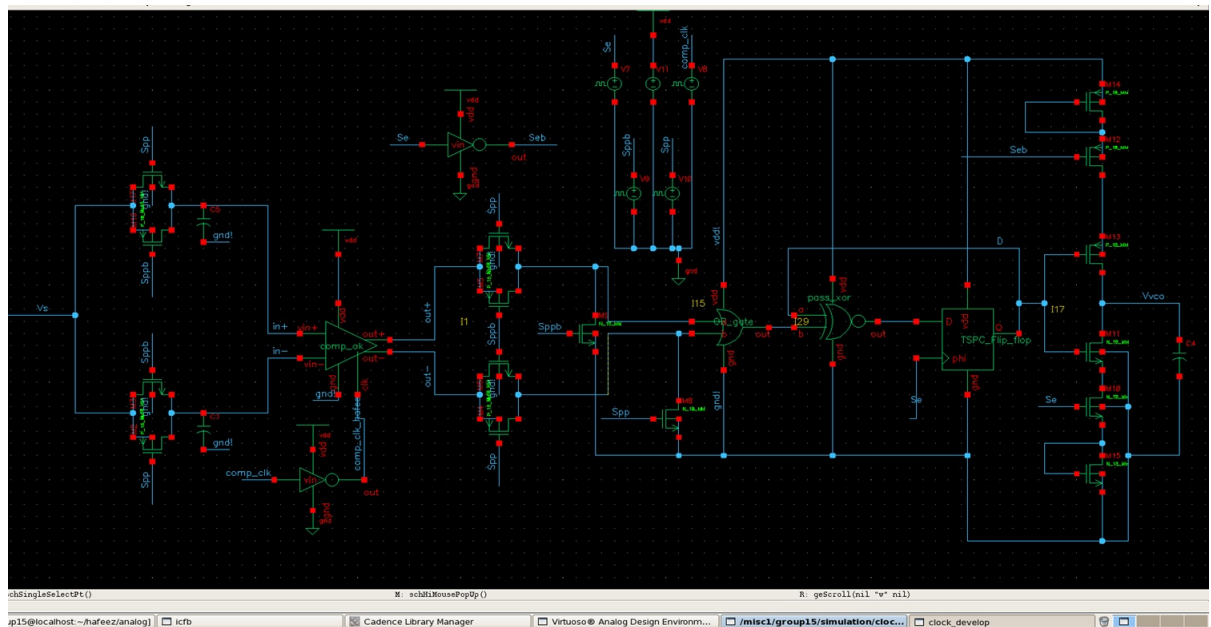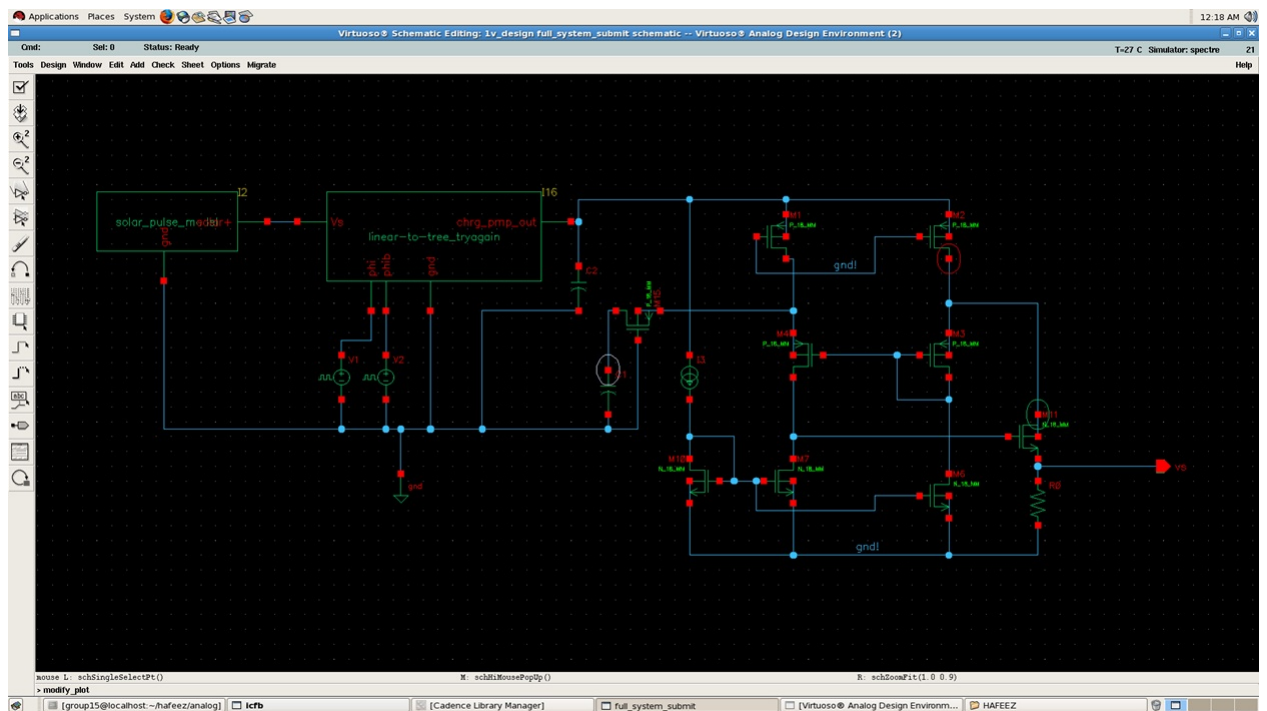
6.3 Simulation results and discussion

The circuit simulations were carried out using CADENCE platform with UMC 0.18 μm CMOS technology. The circuit is implemented as two parts as shown in Fig. 6.6 and 6.7. The first part includes the solar cell model, charge pump and current sensor. In the simulation, it is found that the current sensor fails to work properly at high frequency. The frequency response analysis of current sensor is given in Fig. 6.8. It shows that the current become frequency dependent even before 1MHz. so the performance of the system is limited by the current sensor. The state-of-the-art on-chip current sensors based on sensing current through power MOSFET cannot simultaneously achieve over 90% sensing accuracy and enable the buck regulator operating at a switching frequency beyond 1MHz with low quiescent current consumption. When an internal two-stage amplifier is used in the current sensor to increase the loop-gain magnitude and to improve the sensing accuracy, the speed of the current sensing is limited by the unity-gain frequency (UGF) of the amplifier under low quiescent condition.

Figure 6.9 shows the waveforms of at intermediate stages of circuit section1 (Fig. 6.7) and Fig. 6.10 shows the variation of V_{vco} with V_S. ie as Vs changes, the V_{vco} also changes accordingly to track MPP.

6.4 Conclusions

In principle Hill climbing algorithm is best suited MPPT algorithm for single solar cell systems, the practical implementation faces many difficulties. The current sensor based circuit performs well for high voltage- low current systems where the switching frequency of the power converter can be low (2 MHz). In low voltage-high current systems (eg: single solar cells), the switching frequency requirement of power converter will be high (10-20MHz). However the current sensor for switching power converters fails to work properly in high frequencies. Therefore to implement hill climbing algorithm for micro scale system requires a modification of the current sensor.

44

Figure 6.6: Section 1: charge pump with current sensor

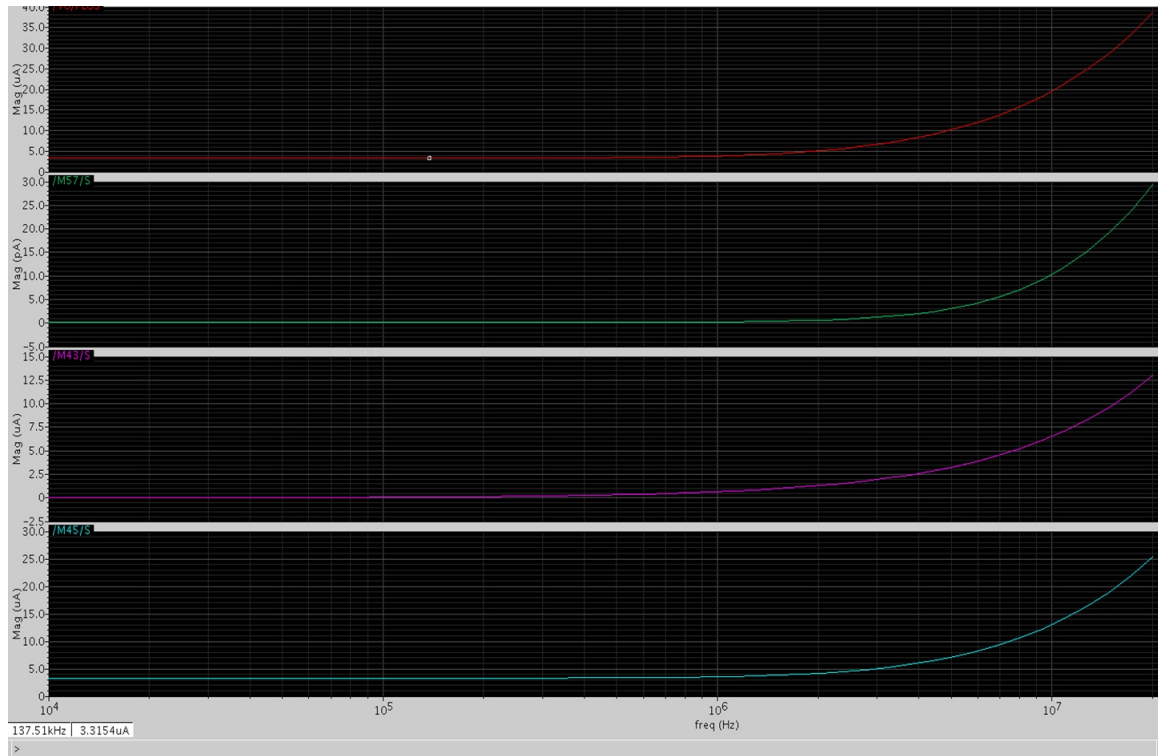

Figure 6.7: Section 2: Decision generation circuit

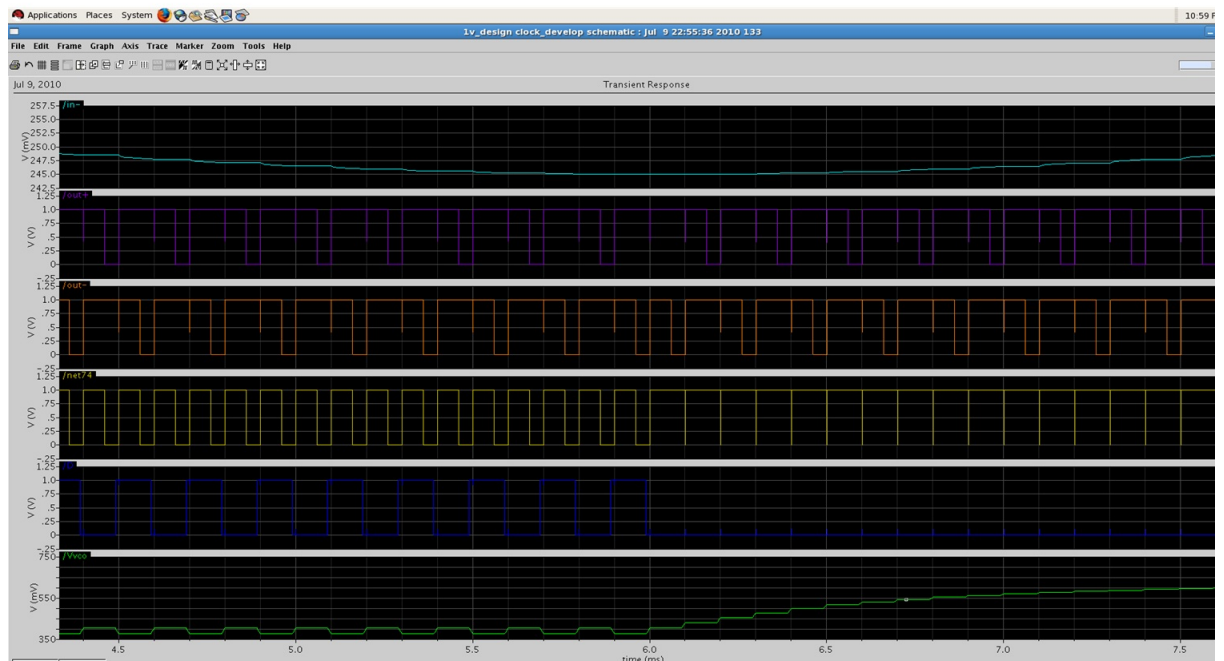Figure 6.8: Frequency response of current sensor

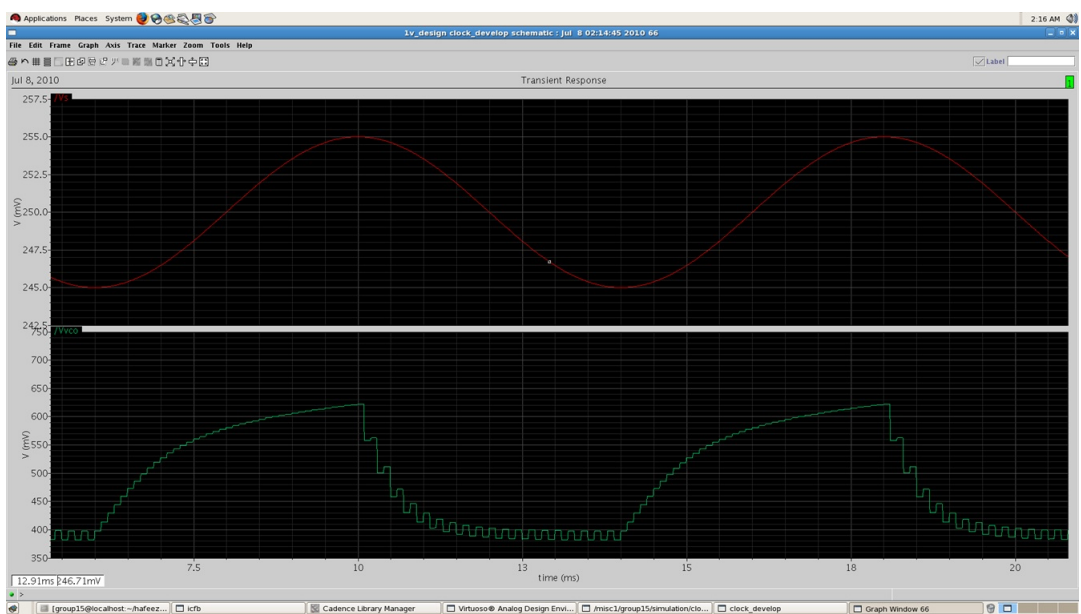Figure 6.9: Simulation results showing the wave forms of V_{check}, V_{action} and V_{vco}

Figure 6.10: V_{vco} variation with V_s

Chapter 7

Design of Feed forward MPPT technique for energy harvesting

7.1   Introduction

The design of an efficient maximum power point tracking schemes for micro-scale energy systems is a challenging research area. There are number of research article came out recently to design MPPT circuit targeting for low power energy harvesting [19, 18]. Most of them uses Fractional Open Circuit method or Hill Climbing method. Efficiency of the referred MPPT circuits [19, 18] expected to be poor for single solar cell system because of the circuit complexity and presence of power hungry circuits. Among them, Hill Climbing algorithm approach can be best fitted structure for single solar cell system, but it has been proved in previous chapter that it fails to function under targeted specification. Therefore, our design goal is to mitigate the problem.

Recently Lu.et al [23] has proposed a theoretical MPP tracking method based on the analysis of the characteristics of solar cell and charge pump. The summery of the method is, by observing that the output of the solar cell is connected to the input of the charge pump, it is possible to derive an expression that relates the optimal operating point of the charge pump to the output voltage of the solar cell. This expression can then be directly implemented using dedicated hardware. The advantage of this approach is that the elimination of explicit current and voltage sensing at the output of the transducer or power converter (hence decreasing hardware cost and power overheads) can be possible. However the hardware implementation of the expression will be very complex and difficult. Therefore we propose an empirical method to overcome the hardware complexity. That will resulted in high accuracy MPP tracking for ultra-low power system.

7.2   System description

The proposed method derives the MPP information from the operating point of solar cell. The functional block diagram of the proposed Feed Forward MPP tracking system is shown in Fig. 7.1. It consists of a solar cell, charge pump, battery and an optimal clock computing circuit. Solar cell converts the light energy to electrical energy and charge pump is used to step up the voltage before storing to battery. The solar cell output is connected to both charge pump and the clock computing block. The impedance matching of solar

cell and charge pump is taken care by the clock computing circuit. The clock computation block will supply optimum frequency to charge pump based on the operating point of the solar cell.
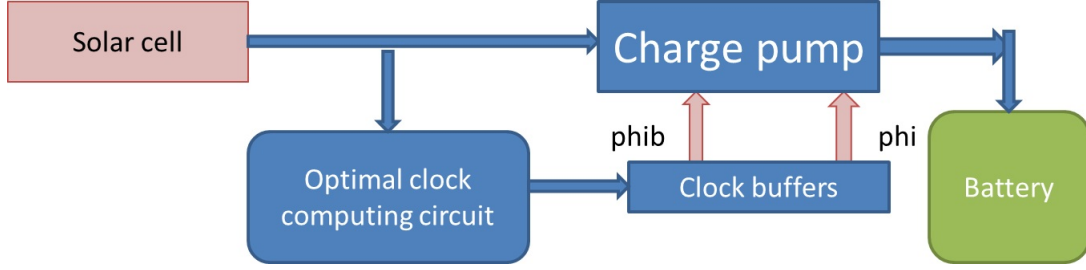

Figure 7.1: Block diagram of proposed Feed Forward based solar energy harvesting system

7.3 Theoretical approach

The aim of the proposed method is to extract the information about optimum clock frequency of charge pump from the operating point of solar cell. For the derivation purpose, we can feed either solar current or voltage as an input to the optimal clock computing unit. The current feeding is not preferable from practical implementation point of view. As it will reduce the output power and it will change the operating point. However, the voltage feeding is most suitable as it will not affect the operating point.

Since in ultra-low power system, the solar MPP and system MPP are different, a combined analysis of solar cell, charge pump and the losses in the system is required to find the relation between solar operating voltage (V_{OP}) and charge pump frequency (F_{clk}). In this approach, the solar cell and the charge pump are modeled in from of an equivalent electrical circuit. In the following section, we have established the relationship by detailed analysis and a modular level sketch is added in Fig 7.2. for derivation purpose.
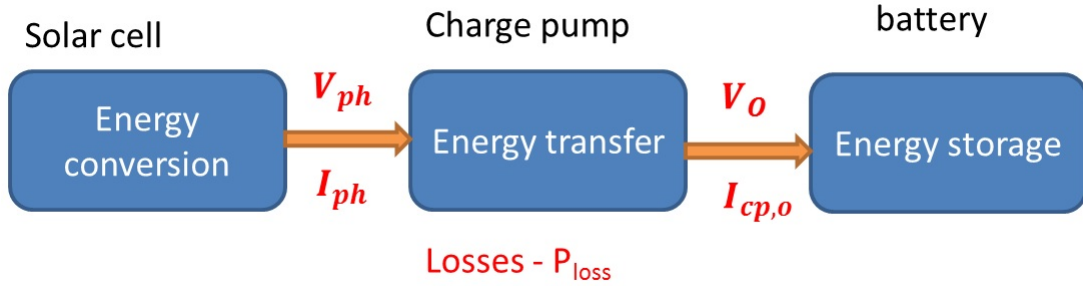

Figure 7.2: Illustration of the inherent processes of energy conversion

7.3.1 Relation between V_{PH} and F_{clk}

For finding the relationship through theoretical derivation, the output current of charge pump is expressed by [20]

$$\mathrm{I}_{cpo} = \frac{1}{N} C f_{clk}[(N+1)\mathrm{v}_{ph} - \mathrm{v}_o] \tag{7.1}$$

Where V_{PH} is the solar cell output voltage, N is the number of stages of the charge pump and C is the charge pump capacitance. Now, since the charge pump steps up the input voltage by (N+1), the input current of charge pump (I_{ph}) can be expressed as

$$\mathrm{I}_{cpo} = \frac{N+1}{N}Cf_{clk}[(N+1)\mathrm{v}_{ph} - \mathrm{v}_o] - i_{loss} \tag{7.2}$$

By considering only the current loss due to reverse current in the charge pump, I_{ph} will be,

$$\mathrm{I}_{cpo} = \frac{N+1}{N}Cf_{clk}[(N+1)\mathrm{v}_{ph} - \mathrm{v}_o] - \sigma F_{clk} \tag{7.3}$$

Where σ is a constant accounting for the reverse current loss and it is depending on the design.

From Eq 7.3,

$$\mathrm{V}_{ph} = \frac{I_{ph}}{\alpha F_{clk}} + \frac{\beta}{\alpha} \tag{7.4}$$

where where

$$\alpha = \frac{(N+1)^2}{N}C \tag{7.5}$$

and

$$\beta = \frac{N+1}{N}CV_0 - \sigma \tag{7.6}$$

Eq. 7.4 shows that the solar cell voltage decreases as the clock frequency of the charge pump increases. This expression is of idealistic nature, the losses (referred in chapter 5) has to include to derive exact relationship, that has described below,

7.3.2 Optimization of the losses

Now, including the switching current loss (P_{swt_total}), conduction current loss (P_{con_avg}) and the biasing current loss (P_{bias}), the total loss in the MPPT is given by

$$\mathrm{P}_{loss\_total} = P_{swt\_total} + P_{con\_avg} + P_{bias} \tag{7.7}$$

Then using Eq 5.5 , Eq 5.12 and Eq 5.13,

$$\mathrm{P}_{loss\_total} = \frac{1}{2}M\frac{I_{on}^2}{\mu C_{ox}\left(\frac{w}{l}\right)\left(V_{gs} - V_{th} - \frac{1}{2}V_{ds}\right)} + \frac{5}{2}MC_{ox}\left(Wl\right)V_o^2F_{clk} + I_{bias}V_{bias} \tag{7.8}$$

To minimize the power loss, the authors [51] differentiated the Eq. (7.5) with respect to the transistor width (W) and the optimized value of W is substituted in Eq 7.5. The optimized power loss is given by

$$\mathrm{P}_{loss\_total} = P_{bias} + MlI_{on}V_o\sqrt{\frac{5F_{clk}}{\mu\left(V_{gs} - V_{th} - \frac{1}{2}V_{ds}\right)}} \tag{7.9}$$

Now substituting F_{clk} from Eq 7.4 to Eq 7.6, the total power loss in terms of solar output voltage is as given below.

$$P_{loss\_total} = P_{bias} + MlI_{on}V_o \sqrt{\frac{5I_{ph}}{\mu\left(\alpha V_{ph} - \beta\right)\left(V_{gs} - V_{th} - \frac{1}{2}V_{ds}\right)}} \qquad (7.10)$$

Since, the effective power (P_0) to the battery for storage is the difference between solar output power and total power losses. The solar output power is given as $V_{ph}I_{ph}$ and the power loss is given in Eq 7.7, then

$$P_0 = V_{ph}I_{ph} - P_{bias} - MlI_{on}V_o \sqrt{\frac{5I_{ph}}{\mu\left(\alpha V_{ph} - \beta\right)\left(V_{gs} - V_{th} - \frac{1}{2}V_{ds}\right)}} \qquad (7.11)$$

To obtain the value of V_{ph} that will deliver maximum power to battery, we maximize the Eq 7.11 with respect to V_{ph}. Substituting the V_{ph} value in Eq 7.4 will give the relation between optimum clock frequency and solar output voltage. The implementation of this expression using dedicated hardware will help to track MPP. However, it has been observed that the implementation through above process is difficult due to the complexity of the equation. Moreover, from solar cell I-V characteristic, it is observed that V_{ph} depends on I_{ph} and it can also expressed as

$$V_{oc} = \frac{nKT}{q}l_n\left(\frac{I_L - I_{ph}}{I_0} + 1\right) \qquad (7.12)$$

Therefore, the differentiation becomes more complex. Even if we able to obtain the result, the relationship will be too complex to realize using dedicated hardware effectively. In following section, we have proposed one empirical method as an alternative.

7.4   Practical implementation

In the proposed alternative approach (Fig. 7.1), the function of the optimum clock computing unit is to provide optimum clock frequency to charge pump based on solar output voltage. Therefore, the function of optimum clock computing unit is equivalent to a voltage control oscillator (VCO), as it is producing a clock with variable frequency based on feeding input voltage. The VCO should able to produce the optimum clock frequency from feeding solar voltage for MPP tracking.

The required characteristic of the VCO is derived through an empirical method. In this method, the optimum operating frequency of charge pump (at MPP) is manually calculated for different light intensities. This can be done by disconnecting the VCO from the charge pump and then vary the operating frequency of charge pump as shown in Fig 7.3.

We have noted the frequency of VCO for maximum output power and the corresponding solar operating voltage (V_{OP}). Repeating this experiment for different light intensities, we will get samples of solar operating voltage and corresponding charge pump frequency. This is the required characteristics of the VCO that can produce optimum clock frequency to charge pump based on operating point of solar cell. Once the required characteristic of VCO is obtained, the designer can design an equivalent VCO that will match the desired characteristic. In this work, an analog VCO is designed to match the characteristics.

The working of the alternative approach can be explained using impedance matching. Assume in the beginning, the charge pump frequency is zero. So the charge pump impedance is infinite. Since this infinite impedance is connected to solar cell, its operating voltage is open circuit voltage (V_{OC}). This voltage is the input to the VCO. So it will produce a frequency higher than optimum frequency because V_{OC} is higher than V_{MPP}. This high frequency will reduce the impedance of charge pump, and then the operating point will shift
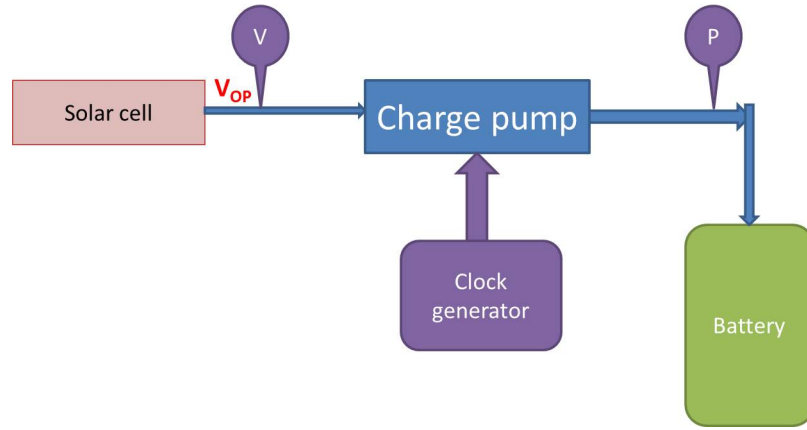
Figure 7.3: Illustration of obtaining the desired characteristics of VCO

towards lower voltage. As a result the VCO frequency will lower down. The system will now move to new operating point. This will continue until it reaches V_{MPP} and deliver maximum power to the output load. Now assume the light intensity has increased. So the impedance of the solar cell reduces and the operating point is disturbed. Since the impedance of charge pump is higher than solar cell, the operating point will tend to shift towards higher voltage. As a result the clock frequency to the charge pump increases. This will reduce the impedance of the charge pump. This process continues until the charge pump impedance become equal to solar impedance. This way the proposed method will track MPP effectively.

7.5 Simulation results and discussion

The circuit is designed in 0.18μm CMOS technology and simulated using Cadence Spectre simulator. The simulation results are shown in Fig. 7.4 to Fig. 7.7. Fig. 7.4 shows the I-V characteristics of solar cell model used in this work. Different light intensities are represented by using different solar current (I_L) in the solar cell model. Fig. 7.5 shows the charge pump output voltage and the clock frequency. The output voltage becomes tangential to the final value after several clock signals. The transistors in the charge pump were designed with different (W/L) ratios as explained in section 5.5

The Table 7.1 shows the maximum power obtained at different light intensities and corresponding frequency. The light generated current (I_L) in the solar model is varied to mimic different light intensities. For each light intensity, the charge pump frequency is varied manually to get the optimum frequency for maximum power transfer. Different values of solar output voltage (for different light intensities) and power obtained and corresponding optimum frequency at which the system works in MPP is tabulated after simulation.

Now we can plot the required voltage - frequency relationship of the VCO and it is shown as blue curve in Fig. 7.6. Select an appropriate VCO and tune its characteristics so that it matches with the required characteristics (blue curve). The red curve in Fig 7.6 shows the designed VCO characteristics and it almost matches with the required curve.

Figure 7.7 shows the power obtained for different light intensities and the tracking ability of the system. We can observe that the frequency of the charge pump varies automatically to track MPP and harvested power depends on light intensity. The comparison of the obtained power with automatic MPPT and manually
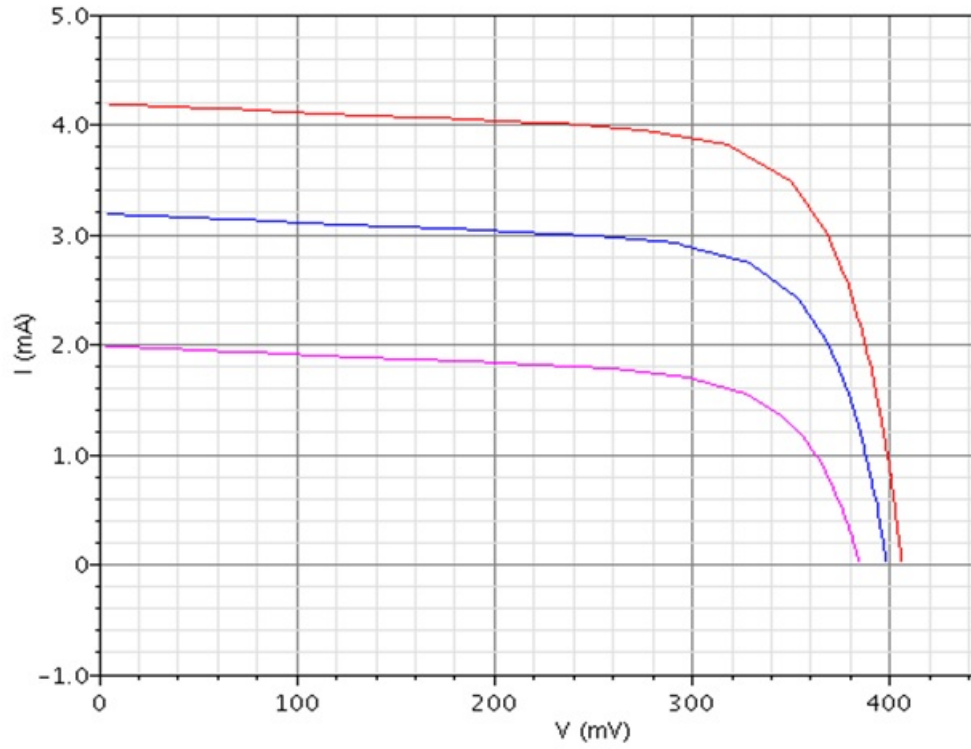
Figure 7.4: Simulated I-V curve using solar cell model

Table 7.1: Characterization of the Feed Forward system

I_L (mA)	Obtained maximum power(μW)	Frequency for max. power(MH_Z)	Solar cell operating voltage at max power (mV)
2	297	7.27	332
2.2	328.3	7.58	334
2.4	358	7.74	336
2.6	391	8.91	339
2.8	416	9.09	345
3	445	9.27	348
3.2	477	10.62	353
3.4	500	11.06	355
3.6	528	11.88	358
3.8	548	12.1	359
4	574	12.33	360
4.2	595	12.55	361

tracking are shown in Table 7.2

7.6 Conclusions

The accuracy of the system depends on how effectively we can design the VCO that matches with the required characteristics. In this method the load is never disconnected from the cell as in FOCV because MPP information is derived from the solar operating point instead of open circuit voltage. This avoids the power loss
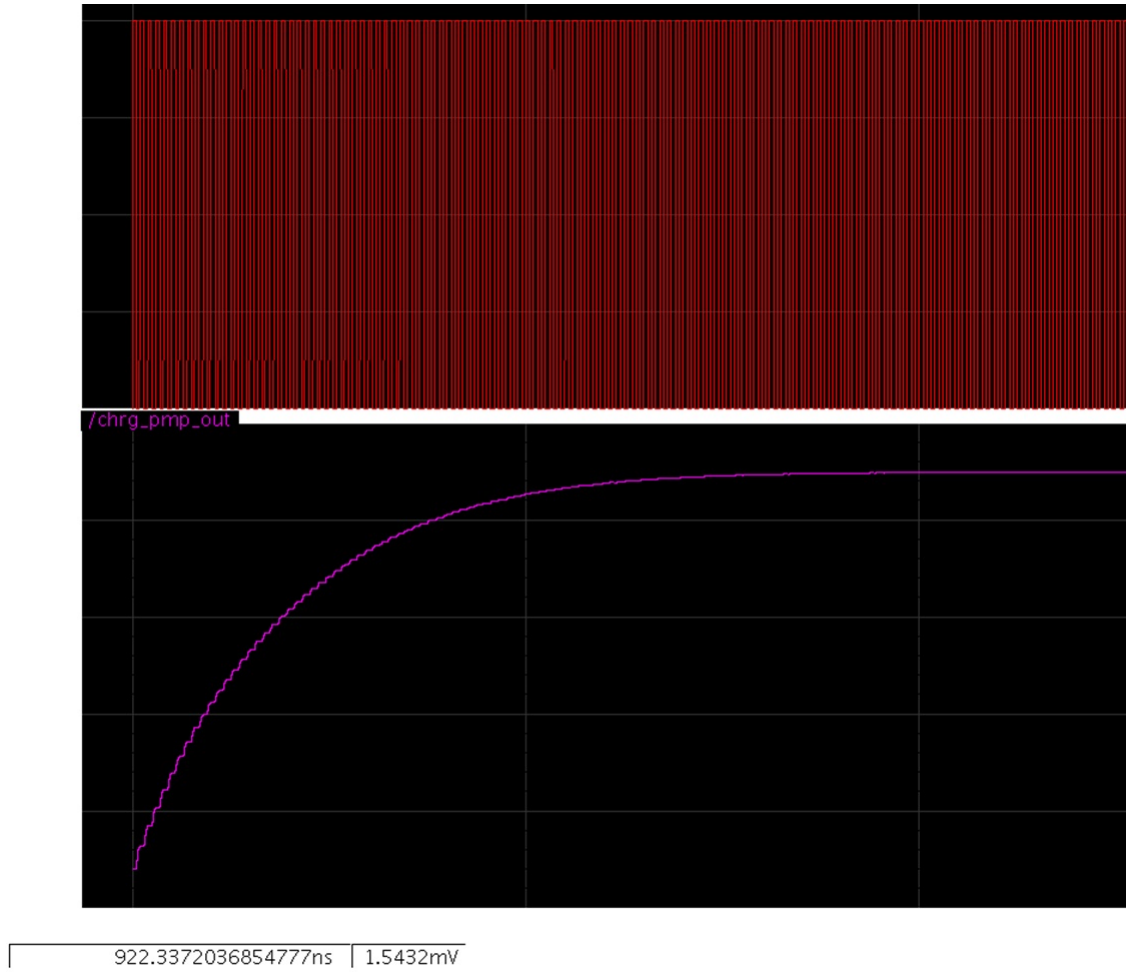
/chrg_pmp_out

922.3372036854777ns   1.5432mV

Figure 7.5: Charge pump output with frequency

Table 7.2: Harvested power comparison

I_L (mA)	Power obtained by manual tracking(μW)	Power Obtained by proposed method (μW)	Percentage error %	efficiency
2	297	296.7	0.1	63.51
2.2	328.3	328.1	0.06	63.05
2.4	358	353.8	1.173	61.71
2.6	391	390.1	0.23	62.30
2.8	416	415.5	0.12	61.23
3	445	437.9	1.59	59.88
3.2	477	476.8	0.04	60.94
3.4	500	499.4	0.12	59.95
3.6	528	527	0.19	59.58
3.8	548	543.3	0.85	57.6
4	574	572	0.34	58.24
4.2	595	592.9	0.35	57.47

due to frequent disconnection from load and also avoids the multiplexing circuit to perform the connection. In hill climbing method, there is a tradeoff between the speed and accuracy of the MPPT. If we increase the
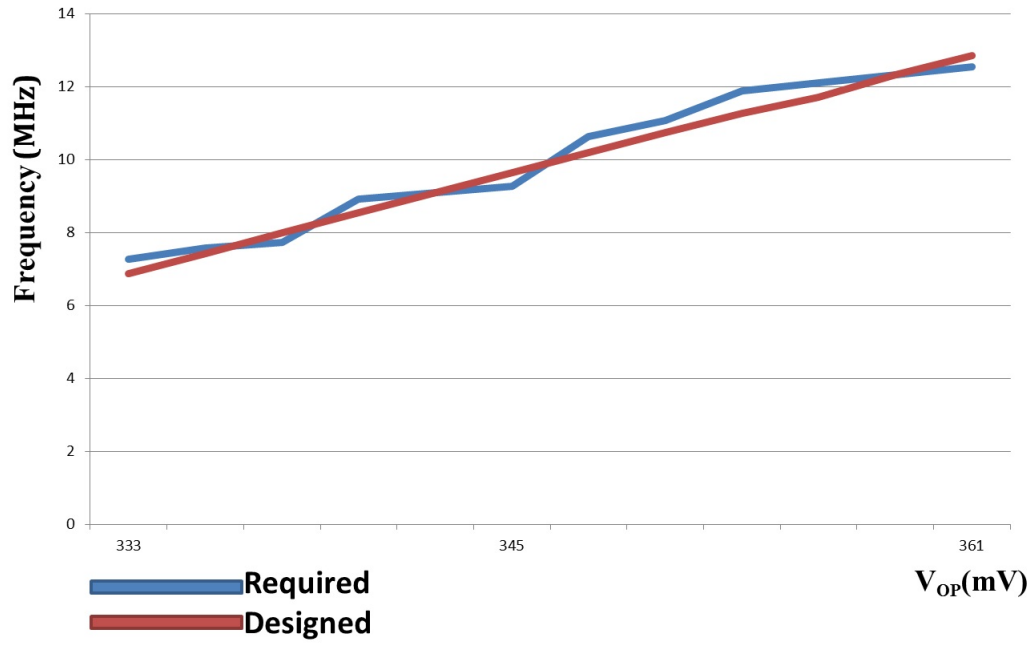
Figure 7.6: Required characteristics and automatically generated characteristics
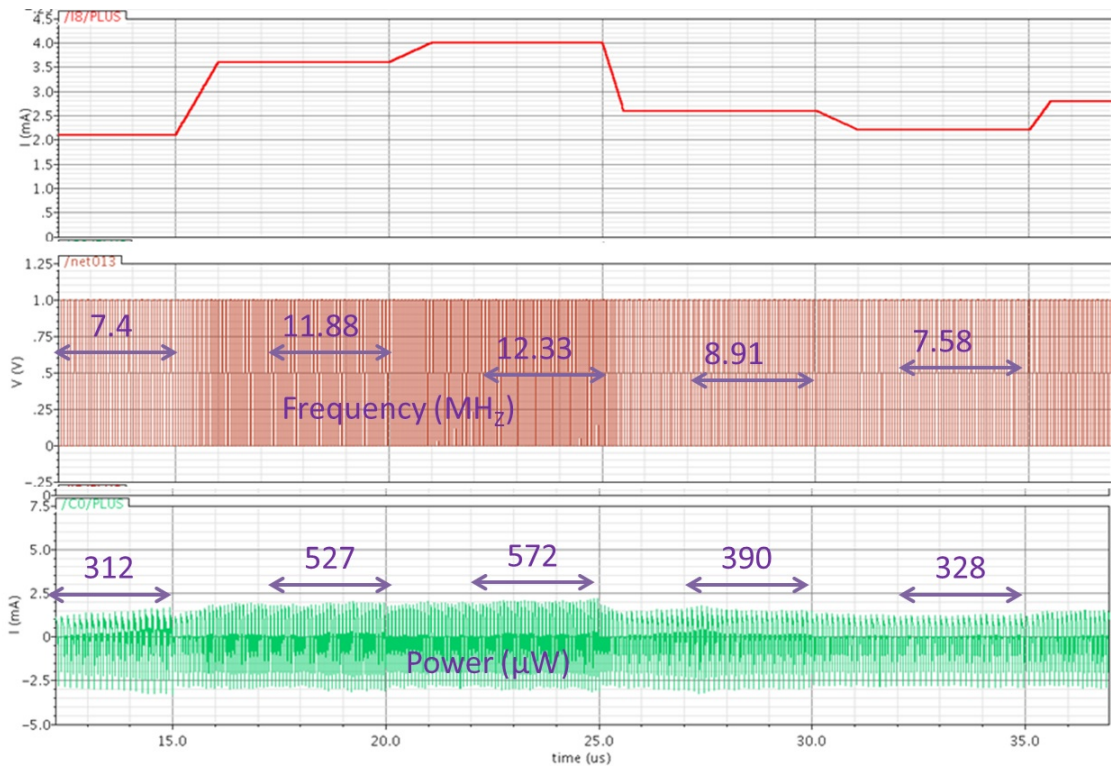
Figure 7.7: Power obtained for different light intensities and corresponding frequency

size of perturbation, the system becomes faster, but less accurate. If the step size is reduced, MPP is more accurate but system will take more time to reach MPP. The proposed system is very faster when compared with

the other methods because it produces optimum clock frequency directly from solar voltage. This method uses minimal hardware among all the MPPT circuit.

Chapter 8

Conclusion and Future Work

8.1 Conclusion

We have presented a comprehensive view on the micro scale energy harvesting system, which can effectively function as energy source for ultra-low power systems. The system offers a perennial power source to low power wireless devices to work completely autonomous. The thesis has emphasized the development of suitable low-power MPPT methods for solar energy harvesting. Analysis of solar cell, charge pump and the power losses are presented. Circuit implementation of Hill climbing algorithm is analyzed and its drawbacks are discussed. A new MPPT method based on feed forward technique is introduced. The proposed method tracks MPP much faster when compared to other methods with high accuracy. The circuits have been designed and performance of the system is verified using 0.18μm CMOS process.

8.2 Future Work

This work can be further carried out as a future scope in order to develop a comprehensive solution for micro scale energy harvesting as follows:

- Tape out of the proposed MPPT system and testing in real environment.

- Develop a startup circuit so that the system works even if the energy buffer is completely dried off.

- Design of high frequency, low power current sensor to establish hill climbing algorithm.

- Design of high efficiency charge pump circuits for energy harvesting applications where input voltage is sub threshold.

- Design of multi-source reconfigurable power management system that enables composition of multiple energy harvesting sources including solar, wind, thermal, fuel and vibration

References

[1] B. Atwood, B. Warneke, and K. Pister. Preliminary circuits for smart dust. In Southwest Symposium on Mixed Signal Design. 2000 87–92.

[2] R. F. Yazicioglu and T. Torfs. Ultra-low-power biopotential interfaces and their applications in wearable and implantable systems. *Microelectronics Journal* 40, (2009) 1313–1321.

[3] V. Raghunathan and P. H. Chou. Design and power management of energy harvesting embedded systems. In ACM/IEEE International Symposium on Low Power Electronics and Design (ISLPED). 2006. 369– 374.

[4] L. Mateu and F. Moll. Review of energy harvesting techniques and applications for microelectronics,. In SPIE Microtechnologies for the New Millennium. 2005. 359–373.

[5] S. Chalasani and J. Conrad. A survey of energy harvesting sources for embedded systems. In Southeastcon, 2008. IEEE pp, 2008. 2008 442–447.

[6] A. Chandrakasan, D. Daly, J. Kwong, and Y. Ramadass. Next generation micro-power systems. In IEEE Symposium on VLSI Circuits. 2008 2–5,.

[7] C. Carvalho and N. Paulino. A MOSFET only, Step-Up DC-DC Micro Power Converter, for Solar Energy Harvesting Applications. In 17th International Conference "Mixed Design of Integrated Circuits and Systems". 2010, 499–504.

[8] J. W. Kimball, T. L. Flowers, and P. L. Chapman. Issues with low input voltage boost converter design. In Power Electronics Specialists Conference, volume 3. 2004 2152– 2156.

[9] D. Li and P. H. Chou. Maximizing Efficiency of Solar Powered Systems by Load Matching. In ISLPED04. 2004 162–167.

[10] E. Esram and P. L. Chapman. Comparison of photovoltaic array maximum power point tracking techniques. *IEEE Transactions on Energy Conversion* 22, (2007) 439–449,.

[11] R. Shepard, M.; Williamson. Very low voltage power conversion. In The 2001 IEEE International Symposium on Circuits and Systems. 2001 289 292.

[12] J. Jeong, X. F. Jiang, and D. E. Culler. Design and Analysis of Micro-Solar Power Systems for Wireless Sensor Networks. Technical Report UCB/EECS-2007-24, EECS Department, University of California, Berkeley 2007.

[13] X. Jiang, J. Polastre, and D. E. Culler. Perpetual environmentally powered sensor networks. In Proceedings of the Fourth International Symposium on Information Processing in Sensor Networks, IPSN 2005, (UCLA, Los Angeles, California, USA),. 2005 463468.

[14] J. Hsu, J. Friedman, V. Raghunathan, A. Kansal, and M. B. Srivastava. Heliomote: Enabling self-sustained wireless sensor networks through solar energy harvesting. In ACM-IEEE International Symposium on Low Power Electronic Design (ISLPED). 2005 .

[15] F. Simjee and P. Chou. Everlast: long-life, supercapacitor-operated wireless sensor node. In Proceedings of the 2006 international symposium on Low power electronics and design, (New York, NY, USA). ACM Press,, 2006 197202.

[16] C. Park and P. Chou. Ambimax: Autonomous energy harvesting platform for multi-supply wireless sensor nodes. In Proceedings of the Sensor and Ad Hoc Communications and Networks. SECON 06.,, volume 1. 2006. .

[17] K. Kobayashi, H. Matsuo, and Y. Sekine. A novel optimum operating point tracker of the solar cell power supply system. In Power Electronics Specialists Conference, 2004. PESC 04. 2004 IEEE 35th Annual, volume 3. 2004. 2147–2151.

[18] D. Brunelli and L. Benini. An efficient solar energy harvester for wireless sensor nodes. In Proceedings of the conference on Design, automation and test in Europe. 2008 104–109,.

[19] H. Shao, C.-Y. Tsui, and W. H. Ki. A micro power management system and maximum output power control for solar energy harvesting applications. In ACM/IEEE International Symposium on Low Power Electronics and Design (ISLPED),. 2007. 298–303,.

[20] C. Lu, S.-P. Park, V. Raghunathan, and K. Roy. Efficient Power Conversion for Micro Scale Energy Harvesting,. In Design, Automation, and Test in Europe (DATE) Conference. 2010. .

[21] H. Y. H. Lam, W. H. Ki, and D. Ma. Loop gain analysis and development of high-speed high-accuracy current sensors for switching converters,. In Proc. IEEE Symp. Circuits and Systems,. 2004 828 831.

[22] M. Du and H. Lee. A Speed- and Accuracy-Enhanced On-Chip Current Sensor with Local Shunt Feedback for Current-Mode Switching DC-DC Converters. In 6th IEEE Dallas Circuits and Systems Workshop on System-on-Chip DCAS 2007. 2007 1–4.

[23] C. Lu, V. Raghunathan, and K. Roy. Micro-scale Energy Harvesting: A System Design Perspective. In Special Session, Asia and South Pacific Design Automation Conference. 2010. 89–94.

[24] C. Lu, V. Raghunathan, and K. Roy. Maximum Power Point Considerations for Micro-Scale Solar Energy Harvesting Systems. In IEEE International Symposium on Circuits and Systems. 2010 .

[25] G. Palumbo and D. Pappalardo. Charge Pump Circuits: An Overview on Design Strategies and Topologies. *IEEE circuits and systems magazine first quarter* 31 –45.

[26] F. Pan and T. Samaddar. Charge Pump Circuit Design. McGraw-Hill Professional,, 2006.

[27] J. Rabaey, J. Ammer, T. Karalar, S. Li, B. Otis, M. Sheets, and T. Tuan. Pico Radios for wireless sensor networks: the next challenge in ultra-low power design. In Solid-State Circuits Conference, 2002. IEEE International Digest of Technical Papers. ISSCC. 2002, volume 1. 2002 200 – 201.

[28] J.-H. Lin and Y.-H. Kao. Wireless temperature sensing using a passive RFID tag with film bulk acoustic resonator. In Ultrasonics Symposium, 2008. IUS 2008. IEEE. 2008 2209 – 2212.

[29] B. Calhoun, D. Daly, N. Verma, D. Finchelstein, D. Wentzloff, A. Wang, S.-H. Cho, and A. Chandrakasan. Design consideration for ultra-low energy wireless micro sensor nodes. *Computers, IEEE Transactions on* 54, (2005) 727–740.

[30] R. Russ. Battery power trade-offs: low voltage or high capacity?. EE Times [online].

[31] P. Bratt. Energy Harvesting for Wireless Sensor Networks. empfasis, pp 1-3. 2011.

[32] W. R. Heinzelman, A. Chandrakasan, H. Balakrishnan, and C. MIT. Energy efficient communication protocol for wireless micro sensor networks. In Proceedings of the 33rd Annual Hawaii International Conference on System Sciences. 2000 10.

[33] R. Szewczyk, A. Mainwaring, J. Polastre, J. Anderson, and D. Culler. An analysis of a large scale habitat monitoring application. In Proceedings of the 2nd international conference on Embedded networked sensor systems, New York,USA. ACM Press, 2004 214226.

[34] S. Kim, S. Pakzad, D. Culler, J. Demmel, G. Fenves, S. Glaser, and M. C. Turon. Health Monitoring of Civil Infrastructures Using Wireless Sensor Networks. In In the Proceedings of the 6th International Conference on Information Processing in Sensor Networks (IPSN '07). ACM Press, 2007 254–263.

[35] S. Roundy, P. K. Wright, and J. Rabaey. A study of low level vibrations as a power source for wireless sensor nodes. *Comput.Commun.* 26, (2003) 1131 1144.

[36] J. A. Duffie and W. A. Beckman. Solar Energy Thermal Processes. Wiley & Sons, 1974.

[37] T. Shears. Data Centers, Power Consumption, and Global Warming Will the Web Crash? Gimmie the Scoop [Online], http://www.gimmiethescoop.com/data-center-power-consumption-globalwarming-will-the-web-crash 2009.

[38] R. Swanson. Developments in Silicon Solar Cells. In IEDM 2007. IEEE Internationa Electron Devices Meeting. 2007 359 362.

[39] S. A. Kalogirou. Solar energy engineering: process and system. elsevier publications, 2009.

[40] http://pveducation.org/pvcdrom/solar-cell-operation/quantum-efficiency.

[41] Texas Instruments TPS61200 low input voltage DC-DC converter, (http://focus.ti.com/lit/ds/symlink/tps61200.pdf).

[42] C. Rodriguez and G. A. J. Amaratunga. Analytic solution to the photovoltaic maximum power point problem. *IEEE Trans. Circuits System.Reg. Papers* 54, (2007) 20542060.

[43] T. L. Nguyen and K.-S. Low. A Global Maximum Power Point Tracking Scheme Employing DIRECT Search Algorithm for Photovoltaic Systems. *IEEE Transactions on Industrial Electronics* 57, (2010) 3456 3467.

[44] J.-T. Wu and K.-L. Chang. MOS Charge Pumps for Low-Voltage Operation. *IEEE JOURNAL OF SOLID-STATE CIRCUITS* 33, (1998) 592–597.

[45] R. Pelliconi, D. Iezzi, A. Baroni, M. Pasotti, and P. L. Rolandi. Power Efficient Charge Pump in Deep Submicron Standard CMOS Technology. *IEEE JOURNAL OF SOLID-STATE CIRCUITS* 38, (2003) 1068–1071.

[46] J. F. Dickson. On-Chip high voltage generation in MNOS integrated circuits using an improved voltage multiplier technique. *IEEE J. Solid State Circuits* SC-11, (1976) 374–378,.

[47] F. Su, W. H. Ki, and C. Y. Tsui. Gate control strateies for high efficiency charge pumps. In IEEE International Symposium on Circuits and Systems (ISCAS). 2005 1907–1910.

[48] P. Favrat, P. Deval, and M. J. Declercq. A high-efficiency CMOS voltage doubler. *IEEE J. Solid State Circuits* 33, (1998) 410– 416.

[49] T. Ying, W. H. Ki, and M. Chan. Area-efficient CMOS charge pumps for LCD drivers. *IEEE J. Solid State Circuits* 38, (2003) 1721–1725.

[50] C. Tsui, H. Shao, W. Ki, and F. Su. Ultra-low voltage power management circuit and computation methodology for energy harvesting applications. In ACM/IEEE Asia and South Pacific Design Automation Conference (ASP-DAC). 2006 96–97.

[51] C. Lu, S. P. Park, V. Raghunathan, and K. Roy. Analysis and Design of Ultra Low Power Thermoelectric Energy Harvesting Systems. In International Symposium on Low Power Electronics and Design. 2010 183–188.

[52] B. H. e. a. Calhoun. Sub-threshold circuit design with shrinking CMOS devices. In IEEE Intl. Symp. On Circuits and Systems (ISCAS). 2009 .

[53] S.-Y. Lee, C.-J. Cheng, C.-P. Wang, and S.-C. Lee. A 1-V 8-bit 0.95mW successive approximation ADC for biosignal acquisition systems. In International symposium on Circuits and Systems, ISCAS 2009. 2009 649 – 652.